DISSERTATIONES
TECHNOLOGIAE
CIRCUMIECTORUM
UNIVERSITATIS
TARTUENSIS
33

PEETER PAAVER

Development of alternative binders based on oil shale fly ash

DISSERTATIONES TECHNOLOGIAE CIRCUMIECTORUM
UNIVERSITATIS TARTUENSIS
33

DISSERTATIONES TECHNOLOGIAE CIRCUMIECTORUM
UNIVERSITATIS TARTUENSIS
33

PEETER PAAVER

Development of alternative binders based on oil shale fly ash

UNIVERSITY OF TARTU
Press
1632

Department of Geology, Institute of Ecology and Earth Sciences, Faculty of Science and Technology, University of Tartu, Estonia.

This dissertation is accepted for the commencement of the degree of Doctor of Philosophy in Environmental Technology at the University of Tartu on 07.09.2021 by the Scientific Council on Environmental Technology of the Faculty of Science and Technology, University of Tartu.

Supervisors: Kalle Kirsimäe, Department of Geology, University of Tartu, Estonia

Martin Liira, Estonian Geological Survey, Department of Geology, University of Tartu, Estonia

Opponent: Miroslav Komljenović, Research Professor, DrSc., Institute for Multidisciplinary Research, University of Belgrade, Belgrade, Serbia

This thesis will be defended at the University of Tartu, Ravila 14A (Chemicum), room 1019 on the 5th of November 2021 at 12:15.

Publication of this thesis was granted by the Institute of Ecology and Earth Sciences, University of Tartu and by the Doctoral School of Earth Sciences and Ecology created under the auspices of the European Social Fund.

ISSN 1736-3349
ISBN 978-9949-03-731-5 (print)
ISBN 978-9949-03-732-2 (pdf)

University of Tartu Press
www.tyk.ee

CONTENTS

LIST OF ORIGINAL PUBLICATIONS

This thesis is based on the following published papers. These papers are referred to in the text by their respective Roman numerals.

I Usta, M.C.; Yoruk, C.R.; Hain, T.; Paaver, P.; Snellings, R.; Rozov, E.; Gregor, A.; Kuusik, R.; Trikkel, A.; Uibu, M. (2020). Evaluation of new applications of oil shale ashes in building materials. *Minerals*, 10, 765. DOI: 10.3390/min10090765.

II Paaver, P.; Paiste, P.; Liira, M.; Kirsimäe, K. (2019). Alkali activation of Estonian Ca-rich oil shale ashes: a synthesis. *Oil Shale*, 36, 214−225. DOI: 10.3176/oil.2019.2S.11.

III Paaver, P.; Paiste, P.; Liira, M.; Kirsimäe, K. (2021). Mechanical activation of the Ca-rich circulating fluidized bed combustion fly ash: development of an alternative binder system. *Minerals* 11, 3. DOI: 10.3390/min11010003.

IV Paaver, P.; Järvik, O.; Kirsimäe, K. (2021). Design of high volume CFBC fly ash based calcium sulfoaluminate type binder in mixtures with ordinary Portland cement. Manuscript submitted to *Materials*.

Author's contribution:

Paper I: The author was responsible for the mineralogical-geochemical characterization of raw materials and hydrated pastes, data collection, and in part contributed to the writing of the manuscript.

Paper II: The author was primarily responsible for planning original research and data collection. He performed metadata analysis and interpretation, the synthesis of analytical data and wrote the manuscript.

Paper III: The author was primarily responsible for planning original research, data collection, the interpretation of analytical results and the synthesis of mineralogical-geochemical-structural and strength data. He coordinated the writing of the manuscript.

Paper IV: The author was responsible for planning original research, data collection, the interpretation of analytical results and the synthesis of data. He coordinated the writing of the manuscript.

1. INTRODUCTION

The Estonian energy sector has historically relied on using Ordovician oil shale, kukersite, occurring at the northern margin of the Baltic Paleobasin in North-eastern Estonia and Northwestern Russia (Bauert and Kattai, 1997). Estonian oil shale, which is one of the best-quality oil shales with a calorific value of 8–9 MJ/kg, has been and still is the largest industrially exploited oil shale resources in the world (Ots, 2006). Until recently, about 70–80% of Estonia's fuel balance was covered by oil shale, whereas more than 90% of electricity was produced at the oil shale burning power plants in 2007 (Statistical Yearbook of Estonia, 2010). The majority (about 80% in the last decades) of mined oil shale is used in thermal power plants for electricity and heat production. The rest of the mined oil shale is used for retorting shale oil and shale-gas, and, before 2020, in cement production as well. While about 20–30 Mt of oil shale was mined annually in the early 1980s (with a production peak at 31 Mt in 1980), mining and the direct use of oil shale at power plants have considerably decreased over the last decades. Nevertheless, ca. 12 Mt of oil shale was mined in 2019 and 9.2 Mt in 2020 (Statistics Estonia, 2019, 2020).

In addition to greenhouse gas emissions, oil shale combustion in power plants and its retorting for shale oil produces a large volume of solid alkaline waste, mainly ash. About 45–53% of its dry mass remains at electric power plants as ash after combustion (Bauert and Kattai, 1997). As a result, 5–6 Mt of Ca-rich alkaline waste is produced in the oil shale industry annually at the current production levels, making Estonia arguably the world's largest solid waste producer per capita with ca. 3–4 tonnes of ash per inhabitant.

Over the last seven decades, the oil shale research has mostly focused on different aspects of oil shale geology, oil shale combustion and retorting technology, and the potential reuse of solid waste from the oil shale industry (Bauert and Kattai, 1997; Kattai et al., 2000; Ots, 2006). In particular, the reuse of waste in the oil shale industry has been the object of numerous studies in past 20 years, especially from the perspective of producing construction materials (Kikas et al., 1999; Raado et al., 2014a; Raado et al., 2014b; Raado et al., 2011; Uibu et al., 2016; Uibu et al., 2021), uses in agriculture (Paat, 2002; Paat and Traksmaa, 2002; Pets et al., 1985), accelerated and natural carbonation for CO_2 sequestration (Berber et al., 2019; Berber et al., 2020; Kuusik et al., 2002a; Kuusik et al., 2002b; Leben et al., 2021; Leben et al., 2019; Uibu et al., 2011; Uibu et al., 2008a; Uibu et al., 2009; Uibu et al., 2008b), the preparation of precipitated carbonate products (Tamm et al., 2017; Uibu et al., 2015; Uibu et al., 2021; Uibu et al., 2007; Velts et al., 2014; Velts et al., 2011; Velts et al., 2009), filler materials in plastics (Uibu et al., 2021), adsorbents for phosphorous removal in constructed wetland systems (Kaasik et al., 2008; Kasak et al., 2016; Kõiv et al., 2010; Kõiv et al., 2012; Kõiv et al., 2009; Liira et al., 2009b; Mõtlep et al., 2007) and the development of alkali-activated materials (Paaver et al., 2016; Paaver et al., 2019—PAPER II; Paaver et al., 2017; Paiste et al., 2019; Paiste et

al., 2017; Paiste et al., 2016). However, despite the tremendous effort put into these studies, the secondary beneficial reuse of oil shale ash (OSA) has been minimal, accounting for less than 2% of the total ash output, even at the current relatively low production rates (Paaver et al., 2021—PAPER III). As a result, millions of tonnes of ash is dumped to large, up to 45 m high waste depositories annually, covering more than 20 km^2 next to the two major power plants (Leben et al., 2019; Mõtlep et al., 2010).

Somewhat larger volumes of the fine fractions of ash feed, collected from the electrostatic filters at the now decommissioned pulverized combustion (PC) boilers, have been successfully used as raw material for the production of Portland clinker. In addition, the coarse fractions of PC ash were used as aggregates in the production of gas-concrete blocks (Raado et al., 2014a) as well as a stabilizing agent in road construction and for liming acidic soils (Kuusik et al., 2006). Since 2004, the high-temperature (>1200–1400°C) pulverized combustion (PC) boilers have been gradually replaced by the more effective and less CO_2 intensive circulated fluidized bed combustion (CFBC) boilers, firing oil shale at 800–850°C (Ots, 2006). Circulated fluidized bed combustion at lower temperature also favours almost complete SO_2 capture by the formation of the solid $CaSO_4$ (anhydrite) phase in a reaction between free CaO and SO_2 (Anthony, 1995).

CFBC technology is the only remaining oil shale firing technology since 2018 when the PC boilers were shut down. It has also been combined with the shale oil retorting solid heat carrier (SHC) technology retorts that use spent shale as a heat carrier. In the Enefit 280 retort, the spent shale and flue gases are additionally combusted at ca. 800°C, producing ash with properties similar to the power plant's CFBC ashes (Paaver et al., 2017).

The change to lower-temperature firing technology and the increased Ca-sulfate content have negatively affected the physical and chemical characteristics of OSA (Pihu et al., 2012; Raado et al., 2014b; Usta et al., 2020—PAPER I). In addition to the increased content of undecomposed carbonate and Ca-sulfate, the formation of Ca-rich phases has moved away from Ca-silicates at the lower operating temperatures towards free lime and silica, resulting in significantly lower cementitious-pozzolanic properties of the CFBC ashes, compared to earlier high-temperature PC ashes. This has already caused problems with ash deposition in ash plateaus (Pihu et al., 2012) and has narrowed down ash reusability (Usta et al., 2020—PAPER I).

The Estonian oil shale industry has reached its final decades. The share of electricity produced at oil shale power plants in Estonia's electricity balance has gradually decreased since 2008, having dropped drastically from about 76% in 2018 to only 40% in 2020 (Statistics Estonia, 2020). The decline in oil shale use at power plants is directly rooted in the carbon dioxide emission allowance trading policy under the European Union Emission Trading Scheme (EU ETS), which has made the use of the fossil fuels, such as Estonian oil shale, uncompetitive in the open energy market. On the other hand, this decline has positively affected Estonia's CO_2 emissions, which are primarily (by more than 70%) generated by burning oil shale (Statistics Estonia, 2020).

This decline in oil shale use is foreseen to continue. In the light of the European Union climate change goals and the recently announced climate-energy package policy and proposals, Estonian government announced in 2021 that oil shale use in power plants will end by 2035 and shale oil retorting by 2045. In addition, the largest energy company in Estonia, Estonian Energy, has declared that oil shale use at power plants will end already by 2030. Nevertheless, Estonia will need to tackle the issues with the utilization of the industry's waste material in the coming decades, as will other countries using oil shale for electricity generation and/or oil extraction, e.g. Jordan with its CFBC power plants, shale-oil retorts in China, etc. However, as mentioned, such solid waste can be considered as potentially valuable secondary raw material to be used for the production of alternative binders and construction materials, accordant to the principles of the circular economy. This category also includes the alkaline solid waste from other industries, such as the ash from biomass combustion, the slag from the steel industry, cement production waste, waste concrete, and the ash from municipal waste incineration (Gosh and Kumar, 2020).

The aim of this thesis is to assess the cementitious properties of oil shale circulated fluidized-bed combustion (CFBC) fly ash, the potential of Ca-rich combustion ash for producing alkali-activated materials and the effects of the mechanical activation on the CFBC fly ash properties, particularly the strength development in hydrated pastes and mortars.

The specific objectives of the dissertation are:

- to characterize the composition of Ca- and S-rich oil shale CFBC ashes and the mechanical properties of their hydrated pastes;
- to review the potential of Ca-rich oil shale ashes for the production of alkali-activated construction materials;
- to study the effects of mechanical activation on oil shale CFBC fly ash paste strength performance, and to develop the pastes and mortars based on mechanically activated CFBC fly ash potentially substituting ordinary Portland cement (OPC).

The thesis puts forward a hypothesis that although raw Ca- and S-rich oil shale ash lacks satisfactory cementitious properties and its high Ca content combined with low silica and aluminium prevents its use as raw material for alkali-activated materials, mechanical activation of oil shale CFBC fly ash makes it suitable for the production of an alternative binder system with properties similar to Ca-sulfoaluminate cements.

2. MATERIALS AND METHODS

2.1. Ash materials

Studied materials were obtained from the oil shale fed boilers at Auvere, Balti and Eesti Power Plants (PP), and Enefit 280 SHC retorting unit including a CFBC boiler. In order to characterize raw ash, different ash fractions separated from the ash flow in Eesti and Auvere PPs CFBC boilers were sampled, including electrostatic precipitator ash (EPA), cyclone ash (CA) and total ash (TA) from power plants, and CA and TA from Enefit 280 plant. At Balti PP CFBC boiler No. 8, average total fly ash (TA) was sampled. For alkali activation, the furnace bottom ash (BA) and cyclone separator ash (CA) materials were obtained from the ash separation system from a boiler operating on PC technology at the Balti Power Plant and from the waste heat boiler system in the Enefit 280 type SHC retort with a CFBC unit (WHB-SCH ash).

For mechanical activation, fresh unhydrated total fly ash material was obtained from the ash separation system at Balti PP CFBC boiler No. 8, which uses oil shale as primary fuel. In this boiler, approximately 60% of total ash is separated as fly ash by means of electrostatic filters. All non-hydrated ash materials that were used in the experiments are representative of the average ash feed at the specific ash separation unit or system.

2.2. Experimental design and sample preparation

The self-cementing properties of raw OSA studied in Usta et al. (2020—PAPER I) were characterized in pastes and mortars with normalized sand prepared with 0.3 water to ash ratio and 0.33 ash to sand ratio for mortars with sand. Pastes were poured into the 40x40x160 mm prisms and compacted with a vibration table. The compacted pastes were first kept in moulds for 48 hours, followed by five days at 60% RH and 20±2°C. Finally they were cured for 28 days at >95% RH and 20±2°C. After 28 days, the uniaxial compressive strength was tested. In Paaver et al. (2021—PAPER III), raw fly ash pastes were mixed using different water to ash ratios (0.35, 0.4, 0.45, 0.5, and 0.55), after which they were poured into 50x50x50 mm moulds in three replicas and placed on a vibrating plate for compaction. Mixing was performed in a laboratory environment at the average ambient temperature of 22±2°C with a relative humidity of 50–60%. The samples were left to cure in moulds under the same conditions for 48 hours, after which they were removed from the moulds and left to cure for 7 and 28 days in an open air environment. In Paaver et al. (in preparation—PAPER IV), raw ash and ordinary Portland cement pastes and mortars containing sand were mixed using different ratios, with a water to ash ratio of 0.4. They were then poured into 30×30×30 mm moulds in three replicas and placed on a vibrating plate for

1 minute. Ordinary Portland cement CM I 42.5R and normalized sand with a grain size of 0.63–2 mm were used.

For alkali activation, ash materials were mixed with a number of different activating solutions: 5 M NaOH, sodium silicate (Na_2SiO_3) solution with SiO_2/Na_2O molar ratio of 2.72 and water content of 47.4% (w/w), and a sodium silicate solution modified by sodium hydroxide addition to SiO_2/Na_2O molar ratio 1.5. The Na2O to ash ratio in all sodium silicate activator solutions was kept at 0.1 (w/w) to normalize the amount of added alkali in the mixtures. After mixing, pastes were poured into cylindrical moulds, either 40 mm in height with a 40 mm diameter (PP ash) or 35 mm in height with a 23 mm diameter (WHB-SHC ash). They were then placed on a vibrating plate for 1 minute. Mixing was performed in a laboratory environment at an average ambient temperature of 22±2°C with a 50–55% relative humidity. Samples were cured under the same conditions in an open air ambient environment for 7 and 28 days for PP ashes and 7, 28 and 90 days for WHB-SHC ash mixtures.

The mechanical activation of ash was conducted in a dry state with a planetary ball mill (RETCH PM100), using ten 20 mm steel grinding balls in a 500 ml steel grinding jar. In Paaver et al. (2021—PAPER III), ash was dry-milled for 2, 3, 4, 6 and 8 minutes at a rotation speed of 500 rpm in 0.5 kg batches. In Paaver et al. (in preparation—PAPER IV), milling was performed for 4 minutes using the same equipment and parameters. Paaver et al. (2021—PAPER IV) found that milling for four minutes was sufficiently effective for ash activation, whereas efficiency started to decrease at 6 and 8 minutes, with the material starting to stick to the sides of the milling container.

The pastes of activated ash studied in Paaver et al. (2021—PAPER III) were mixed with various water/ash ratios (0.35, 0.4, 0.45, 0.5, and 0.55), after which they were poured into 50×50×50 mm moulds. Mixtures of mechanically activated fly ash, ordinary Portland cement and sand (Paaver et al., in preparation—PAPER IV) were mixed at a water to ash/cement ratio of 0.4, after which they were poured into 30×30×30 mm moulds. All mixtures were made in three replicas and placed on a vibrating plate for 1 minute for compaction. Mixing was performed in a laboratory environment at an average ambient temperature of 22°C with a 50–60% relative humidity. Samples were then left to cure under the same conditions in an open air environment for 7 and 28 days. Ash mixtures that were activated by 4 minutes of milling were also left to cure for 90 days in Paaver et al. (2021—PAPER III). Ordinary Portland cement CM I 42.5R and normalized sand with a grain size of 0.64–2 mm were used for mixing with mechanically activated fly ash.

2.3. Analytical methods

The particle size analysis of raw and mechanically activated ash was performed using the laser diffraction particle size analyser Malvern Mastersizer 3000+ by Hydro EV and Horiba Laser Scattering LA-950. Ethanol was used as a dispersant and the samples were continually ultrasonicated during measurements. The

specific surface area was measured by BET analysis using Micrometrics Flex3 and Kelvin 1042 sorptometers.

The uniaxial compressive strength of pastes was measured under continuous loading (20 kPa s^{-1}) until the specimen broke in three replicas with Matest Servo-plus Evolution press in Paaver et al. (2021, in preparation—PAPERS III, IV) and on Toni TechnikD-13355 with load rate of 4 kPa s^{-1} in Usta et al. (2020—PAPER I).

The chemical composition of raw materials was determined by means of X-ray fluorescence spectrometry on a Rigaku Primus II XRF spectrometer using the SQX quantification model with RSD better than 5%. The loss on ignition (L.O.I.) of the samples was determined by heating them at 950°C for two hours. The thermogravimetric (TGA) and differential thermal analysis (DTA) was performed on an STA 449 F3 Jupiter thermal analyser in Al_2O_3 crucibles powdered samples which were first dried at 70°C. The samples were heated from 40 to 1025°C at a rate of 10°C min^{-1} in a N_2 flow of 60 ml min^{-1}.

The Attenuated Total Reflectance-Fourier transform infrared spectroscopy (ATR-FTIR) patterns of raw ash and various pastes were measured by using a „Smart Orbit“ diamond ATR-microanalysator attached to a Thermo Scientific Nicolet 6700 FT-IR spectrometer with CsI optics and DLaTGS detector. Transmittance IR spectra were collected from 225–4000 cm^{-1} at a resolution of 4 cm^{-1} with 128 or 256 scans per sample.

Isothermal calorimetry was performed using micro reaction calorimeter μRC from Thermal Hazard Technology (THT) to measure the heat released during the hydration of activated CFBC fly ash and OPC mixture pastes. The pastes were made with a water/solid ratio of 0.4. Measurements were taken at room temperature over a period of 24 h for mixtures and over 14 days for the pure activated fly ash paste.

The mineral composition of raw ash and pastes was determined after 7, 28 and 90 days in selected samples by means of X-ray diffraction (XRD) analysis on a Bruker D8 Advance diffractometer in randomly oriented pressed powder samples, using Ni-filtered Cu*K*α radiation and LynxEye linear detector over the 2–70°2θ region. The mineral composition of samples was interpreted and modelled using the Rietveld algorithm based code Topaz 4.0. Amorphous phase (glass) content was determined by spiking the samples with 10 wt% ZnO prior to measurement. The amorphous phase content was calculated from the difference between the added and measured ZnO spike, assuming that the apparent lower ZnO content is caused by the adsorption of X-rays by the amorphous phase. The relative error of quantification was better than 10% for major phases (>5 wt.%) and better than 20% for minor phases (<5 wt.%).

The microstructure and chemical composition of raw ash and pastes were investigated using Zeiss EVO15MA SEM with Oxford X-MAX energy-dispersive detector. Samples were examined in freshly broken surfaces in high vacuum mode with 4–5 nm thick Pt coating and in polished slabs with 10 nm thick carbon coating.

3. RESULTS AND DISCUSSION

3.1. Self-cementing properties of the raw CFBC fly ash

The oil shale ash formed in CFBC boilers is characterized by varying grain size and BET specific surface area (Usta et al., 2020—PAPER I; Paaver et al., 2021—PAPER III). The finest mean grain size, 20 to 45 µm, is characteristic to power plant electrostatic precipitator filter and total fly ash fractions (Fig. 1). The BET specific surface area varies from 2.3 to 6 $m^2 g^{-1}$ in these ash fractions, being on average the highest (4.3 $m^2 g^{-1}$) in electrostatic precipitator filter fly ash from the Eesti PP CFBC boiler system (Fig. 2). The mean grain sizes of CA and TA from the CFBC boiler at Enefit 280 retort range from 21 to 35 µm (one outlier sample at 280.8 µm) and 31 to 37 µm, respectively, while the BET specific surface area for WHB-SHC TA is considerably lower (1.7–2.5 $m^2 g^{-1}$) than that of CA from the same ash removal system, averaging at 5.5 $m^2 g^{-1}$ (Figs 1, 2).

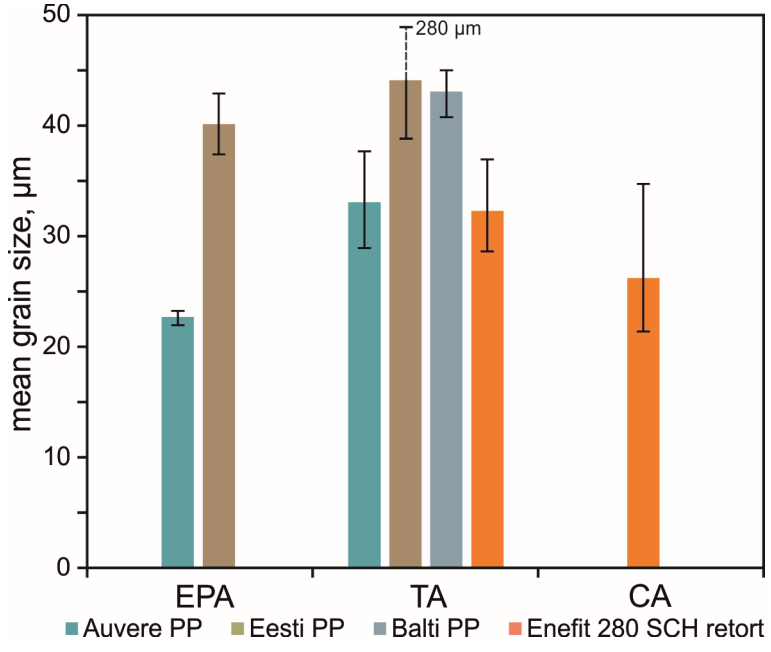

Figure 1. The mean grain size of studied power plants' (PP) and Enefit 280 solid heat carrier (SCH) retort ashes. Electrostatic precipitator (EPA), total fly ash (TA) and cyclon ash (CA) fractions (Usta et al., 20020—PAPER I; Paaver et al., 2021—PAPER III).

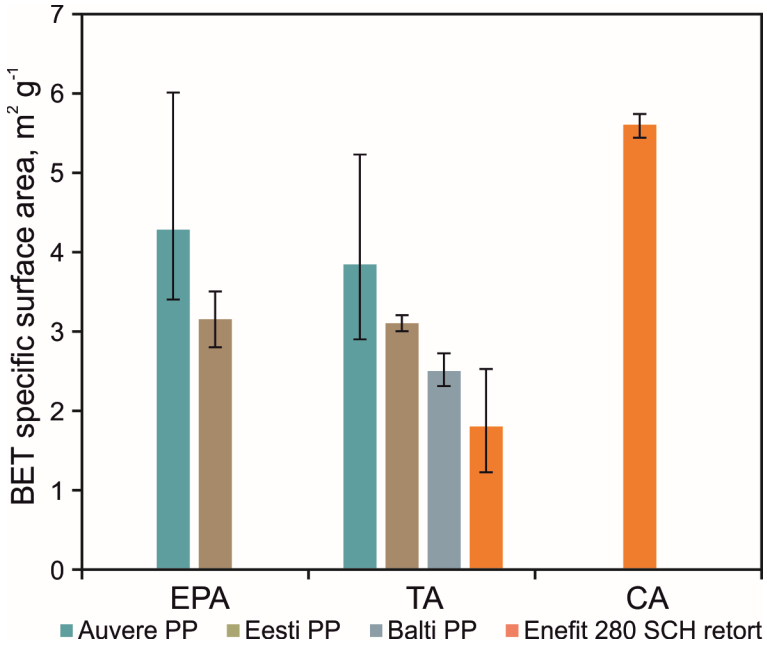

Figure 2. The BET specific surface area of studied power plants' (PP) and Enefit 280 solid heat carrier (SCH) retort ashes in electrostatic precipitator (EPA), total ash (TA) and cyclon ash (CA) fractions (Usta et al., 20020—PAPER I; Paaver et al., 2021—PAPER III).

The mineral composition of the crystalline phases of oil shale ashes (see Fig. 5 and 6 in Usta et al., 2020—PAPER I, and Figs. 4 and 7 in Paaver et al., 2021—PAPER III) is dominated by terrigenous primary silicate phases, which remained largely unaltered during firing: quartz (10–20 wt%), K-feldspar (10–15 wt%), and K-mica (5–15 wt%). In contrast to high-temperature PC ashes where the decarbonization was nearly complete and both calcite and dolomite were absent, CFBC ashes are characterized by incomplete decarbonization (Bityukova et al., 2010; Kuusik et al., 2012), as evidenced by the presence of residual calcite in varying amounts (10–25 wt%). In some samples, dolomite was detected as well, although dolomite already starts to decompose at temperatures exceeding 550°C (L'vov, 2007). The TA from the CFBC boiler at Enefit 280 retort had the highest content of calcite, as well as residual dolomite (Fig. 6 in Usta et al., 2020—PAPER I).

Varying amounts of the periclase (MgO) were detected in all ash types. It is formed by the thermal dissociation of dolomite, and also lime (CaO_{free}) is present after dolomite and partial calcite decomposition . CaO_{free} content is the highest (10–25 wt%) in the finest ash fractions, but it is nearly absent in the TA from the Enefit 280 unit. In addition, due to the effective desulphurization of flue gases, CFBC fly ash is rich in Ca-sulphate (anhydrite, on average 8–10 wt%). Finally, varying amounts (7–22 wt% of crystalline phases) of secondary Ca- and Ca-Mg

silicates (belite—C2S, akermanite and merwinite) forming in boilers by reactions between CaO_{free}, MgO and silica are present in all studied CFBC ash types. The estimated amount of amorphous Ca-Al-Si glass phase in CFBC fly ash varies between 15–20 wt%.

Similar to the mineral composition, the chemical composition of OSAs is variable depending on the ash separation point from the overall ash flow (Usta et al., 2020—PAPER I; Paaver et al., 2021—PAPER III). SiO_2, CaO, Al_2O_3 and mineral CO_2 constitute about 85% of the composition in total. CaO content varies between 27 to 41 wt%, while the content of SiO_2 typically varies between 24–36 wt%. This does not apply to the total ash from Enefit 280 unit, which is characterized by a SiO_2 content of ca. 17 wt%. At the same the Enefit 280 ash is characterized by high content of residual carbonate evidenced by the highest LOI value at 27 wt%. The contents of Al_2O_3, MgO and Fe_2O_3 remain in the range of 5–10, 5–9 and 2–8 wt%, respectively. SO_3 content is particularly high, which is typical of CFBC ashes, varying between 4–9 wt% (Usta et al., 2020—PAPER I; Paaver et al., 2021—PAPER III).

After 7 days of curing, the uniaxial compressive strength of raw CFBC ash pastes yielded the highest average strength value (12.2 MPa) in pastes made with the EPA collected at Auvere PP, while the TA from the same plant showed an average compressive strength of 10.8 MPa (Fig. 3) After 28 days of curing, the EPA from Eesti PP produced the compressive strength of nearly 9 MPa, while the TA from Eesti PP and Balti PP showed values 6.3 and 4.9 MPa, respectively (Fig. 3, Usta et al., 2020—PAPER I; Paaver, et al., 2021—PAPER IV). In contrast, the TA collected from the Enefit 280 boiler reached only 0.4 MPa in compressive strength, even though the CA from the same plant showed comparable performance with the TA from Eesti and Balti PPs (Fig. 3). Similarly, Paaver et al. (2017) reported that the compressive strengths of hydrated Enefit 280 WHB-SCH ash was 3.5 and 3.7 MPa after 7 and 28 days of curing, respectively. Maximum compressive strength in raw ash paste using TA from Balti PP yielded 9.5 MPa after 90 days (Fig. 6 in Paaver et al., 2021—PAPER III).

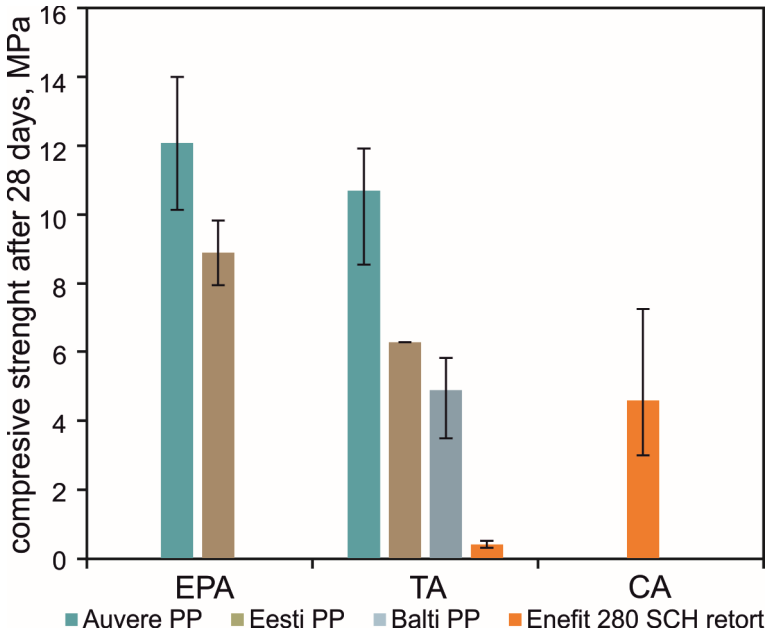

Figure 3. The uniaxial compressive strength of studied power plants' (PP) and Enefit 280 solid heat carrier (SCH) retort ashes. Electrostatic precipitator (EPA), total fly ash (TA) and cyclon ash (CA) fractions (Usta et al., 20020—PAPER I; Paaver et al., 2021—PAPER III).

The self-cementitious properties of raw oil shale ash are controlled by their chemical composition and fineness (specific surface), especially in which regards the content of free CaO and portlandite, secondary Ca/Mg silicates, Ca-sulphate and pozzolanic properties of Ca-Al-Si glassy phase (Usta et al., 2020—PAPER I). Earlier studies have shown that in 7 days the fly ash pastes from now decommissioned PC boilers reached a compressive strength 16 MPa, compared to the 4 MPa strength in CFBC fly ash pastes (Arro et al., 2009; Pihu et al., 2012). This difference is directly related to the content of potential binding phases. The high-temperature PC ensured the complete thermal dissociation of the carbonate phases, as well as vigorous reactions between free CaO and silicate phases, resulting in the formation of multitude potential binding phases—free CaO, belite (β-$CaO{\cdot}SiO_2$) and amorphous glass. These accounted for about 70–80% of the phase composition in the fine fractions of PC ash collected at electrostatic precipitator filters, but the content of these phases was already as high as 50–60% in the coarse-grained bottom ash fractions of the PC ash (Bityukova et al., 2010). This is at least two times higher than the content of reactive phases in CFCB ashes, forming at the temperatures of 800–850°C (Bityukova et al., 2010; Kuusik et al., 2005; Paaver et al., 2021—PAPER III; Usta et al., 2020—PAPER I). In addition to the significantly lower free CaO content in CFBC ashes (15–20 wt% compared to 30 wt% in PC ash), the amount of secondary Ca-silicate phases and amorphous glass phase is at least twice as low in low-temperature CFBC ashes,

pointing at their lower pozzolanic potential. As expected, the least reactive ashes, particularly the TA from Eenfit 280 CFBC boiler with a high content of residual carbonate minerals and the lowest free CaO and secondary Ca/Mg-silicate phases, showed the weakest self-cementitious properties.

With the exception of Enefit 280 CA, the specific surface area and the final compressive strength of the CFBC ash pastes show an excellent positive correlation (Fig. 4) after 28 days, emphasizing the importance of ash fineness in regard to its mechanical properties.

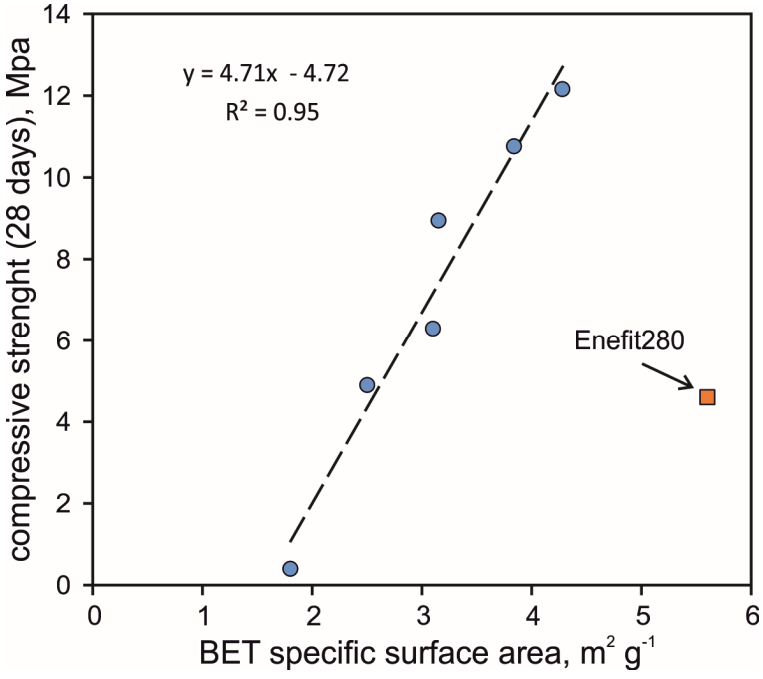

Figure 4. The correlation between BET specific surface area and the uniaxial compressive strength of the studied power plants' (PP) and Enefit 280 solid heat carrier (SCH) retort ashes (Usta et al., 20020—PAPER I; Paaver et al., 2021—PAPER III).

During the hydration of raw oil shale CFBC ash and self-cementitious strength development, the slaking of lime, which leads to the formation of Ca-hydroxide (portlandite), is the fastest reaction, occurring over the first 24–48 hours. However, its subsequent carbonation by CO_2 uptake can go on for decades, depending on carbon dioxide availability (Leben et al., 2019; Liira et al., 2009a; Mõtlep et al., 2010). In the next stage, the dissolution of Ca-sulphate phase (anhydrite) and the establishment of alkaline pore solution initiate the precipitation of ettringite ($Ca_6Al_2(SO_4)_3(OH)_{12}\cdot 26H_2O$), followed by the formation of hydrocalumite ($Ca_2Al(OH)_7\cdot 3H_2O$) and gypsum ($CaSO_4\cdot 2H_2O$) (Kuusik et al., 2012; Liira et al., 2009a; Mõtlep et al., 2010). In addition, Leben et al. (2019) have shown that in ash depository materials composed mainly of PC

ashes, the hydration of secondary Ca-silicate minerals, such as belite (C2S) and Si-Ca-Al glassy phases, can form a C-S-H type semiamorphous phase that provides an additional binding capacity to the oil shale ash sediment, at least in the long term. However, in CFBC ashes, the binding properties seem to be controlled mainly by free CaO and its hydration/carbonation, as well as the precipitation of secondary Ca(Al)-sulphate-hydrate phases gypsum and hydrocalumite, particularly ettringite. However, in raw CFBC ash they do not appear to produce as good self-cementing properties as in high-temperature PC ashes. Hence, the chemical and/or mechanical modification of CFBC ash is required in order to enhance its cementitious properties and widen its usability in construction applications.

3.2. Alkali activation of the oil shale ash

Chemical activation of oil shale ash by alkali solutions is one of the viable options for increasing the sustainable usage of oil shale ashes in the construction industry (Paaver et al., 2019—PAPER II). Alkali-activated materials represent a novel and environmentally friendly binder system, where the cementitious Al-Si binder is formed through the alkali activation of silicate precursors. Alkali-activated materials can have very different compositions and origins. They include, for example, geopolymers which constitute a subset of alkali-activated materials with a 3-dimensional aluminosilicate binder phase structure (Davidovits, 2011). Such materials can be used to produce mortar and concrete with strength properties comparable to OPC and high fire and acid resistance (Duxson et al., 2007).

Raw source materials for such substances can be of very different nature. Both natural or industrial aluminosilicate raw materials can be used for alkali activation (Davidovits, 2011). However, the chemical and physical-mechanical properties of raw materials, as well as the manner of their activation affect the structural-chemical-physical properties of the final product.

In addition to slags from the metallurgical industry and waste glassy products, combustion fly ashes can be used as a raw material for alkali-activated products as well. On one hand, the “classical” geopolymers are based on aluminosilicate raw materials, such as clay (kaolinite) and aluminosilicate rich fly ashes, for instance class F ashes rich in Si and Al that form strong aluminosilicate polymer networks upon alkali activation (Davidovits, 2011; Luukkonen et al., 2018; Zhang et al., 2014a; Zhang et al., 2014b). On the other hand, slags with high CaO content develop cementitious calcium-silicate-hydrate (C–S–H) and calcium-aluminium-hydrate (C–A–H) phases that are formed in the course of OPC hydration as well (Guo et al., 2010a; Mijarsh et al., 2015).

It should be, however, noted that that high Ca content, as in the OSA, is not typical of geopolymer structures forming raw materials, where mechanical strength is provided by the formation of a hydrous alkali aluminosilicate structure, composed of tetrahedral silicate networks, where Al^{3+} partly substitutes

the Si^{4+} while the resulting negative charge is stabilized by an alkali cation (Davidovits, 2011).

Oil shale ash corresponds to the class C fly ashes, characterized by CaO content >20 wt%. However, the CaO content of Estonian oil shale ash is even higher, varying between 30 and 50 wt%, while it is usually between 1 and 20 wt% in other materials used for creating geopolymers (Guo et al., 2010a; Mijarsh et al., 2015). As the result of high Ca content, the composition of Estonian oil shale power plant (PP) and SHC ashes is considerably different (Fig. 5) from the raw materials typically used for alkali activation (Paaver et al., 2019—PAPER II).

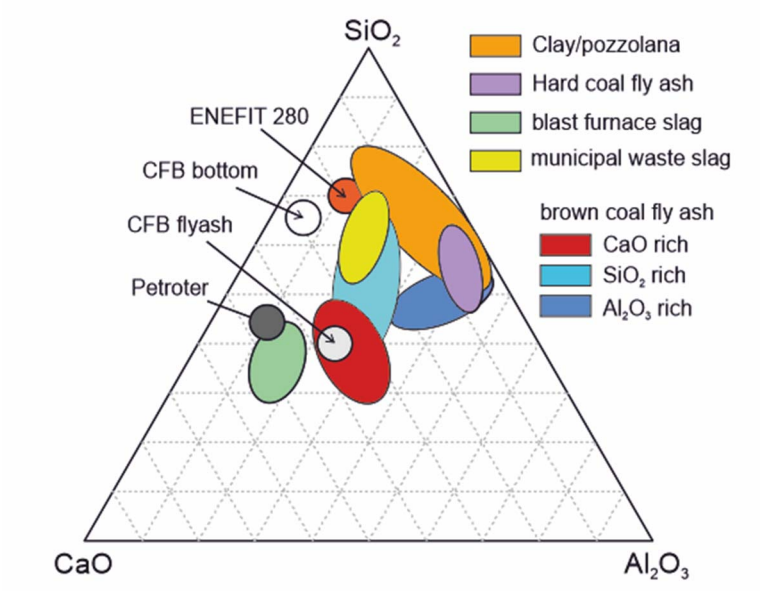

Figure 5. The classification of potential raw materials used for geopolymers on a CaO-SiO_2-Al_2O_3 ternary plot, modified after Buchwald et al. (2005). From Paaver et al. (2019—PAPER II).

Another peculiarity of oil shale PP and SHC ashes is that, compared to other raw materials, they have a significantly lower content of Al_2O_3 (<10 wt%). Duxcson and Provis developed a classification system for geopolymer aluminosilicate source materials based on the molar contents of silica, alumina, and combined network modifiers based on charge-balancing capacity. In this system, the network modifier content is used to quantify the relative amount of alkali and alkali earth metals (Ca^{2+}, Mg^{2+}, Na^{+}, K^{+}) present in fly ash (Duxson and Provis, 2008). Estonian oil shale ashes fall off the compositional fields of other raw materials, including (meta)kaolin clay, F- and C-type fly ashes (Fig. 6), mainly because of their lower Al content (Paaver et al., 2019—PAPER II). This compositional characteristic is enough to cause the formation of strong aluminosilicate polymer networks to be inhibited in the development of uniaxial strength.

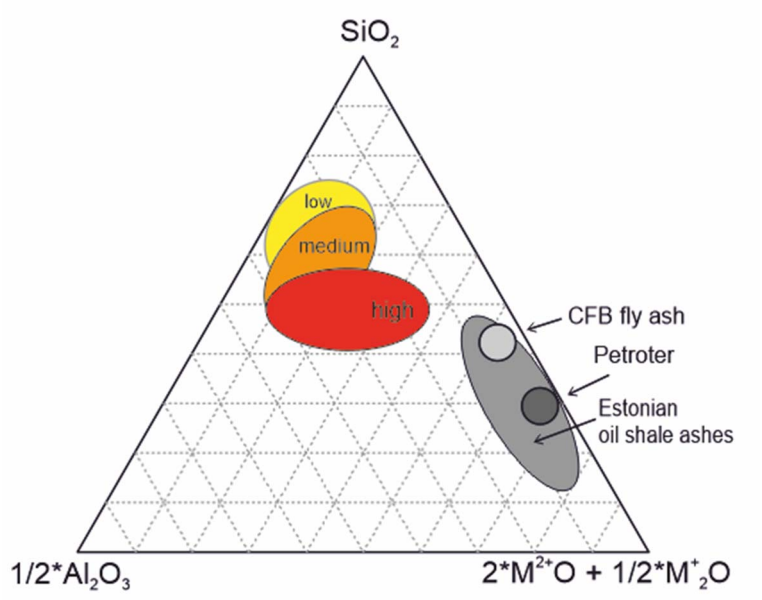

Figure 6. A ternary plot showing the relationship between geopolymer compressive strength and fly ash oxide composition. $M^{+/2+}$ stand for the relative amount of alkali and alkali earth metals. Modified after Aughenbaugh et al. (2015). (Paaver et al., 2019—PAPER II)

Theoretically, the elevated content of alkali elements (*i.e.*, network modifiers), as that of OSA, has been shown to effectively balance the negative charge developed in Al substituted tetrahedral Si networks, resulting in the formation of stronger geopolymers (Duxson and Provis, 2008). However, the uniaxial compressive strengths of alkali-activated oil shale PP and SHC ashes remained relatively lower (typically <10 MPa, reaching maximum 12 MPa after 90 days of curing using SHC oil shale ashes), even though the spectroscopic analyses using ATR-FT-IR and ^{29}Si MAS-NMR analysis of OSA activated with NaOH, Na-silicate and Na-silicate/NaOH showed that the polymerization processes indeed occurred (Paiste et al., 2019; Paiste et al., 2017; Paiste et al., 2016). However, a C–(A)–S–H type (Na)-Ca-Al-Si gel phase developed instead of the typical Si-Al framework (Paiste et al., 2019; Paiste et al., 2017; Paiste et al., 2016). Moreover, ^{29}Si MAS-NMR analysis suggested that the polymerized silicate structures in the alkali-activated PP ashes are represented by one-dimensional structures, lacking branching chains and cross-linking tetrahedral structures. The latter was formed in activated SHC ashes and is characteristic of a three-dimensional geopolymer structure, but the formation of such structures did not improve the mechanical performance of the activated material much, when compared to ash hydrated with plain water (Paaver et al., 2019—PAPER II; Paiste et al., 2019).

Although the length of the polymerized chains increased with the aging of Na-silicate and Na-silicate/NaOH activated ashes (Paiste et al., 2019; Paiste et al., 2017; Paiste et al., 2016), uniaxial compressive strengths of the test specimens

were reduced in aged samples, possibly due to the dry shrinkage and deterioration of the polymeric product induced by excessive calcium and high pH of the mixtures, leading to the precipitation of $Ca(OH)_2$ and its carbonation (Paaver et al., 2016; Paaver et al., 2017). This suggests that even if a longer curing period enables the development of the structurally more polymerized aluminosilicate binder phase, the samples' coherence is lost (Paaver et al., 2016; Paaver et al., 2017; Paiste et al., 2017).

Overall, these studies (Paaver et al., 2016; Paaver et al., 2019—PAPER II; Paaver et al., 2017; Paiste et al., 2019; Paiste et al., 2017; Paiste et al., 2016) suggest that Estonian oil shale ashes do not show sufficient potential for geopolymerization. This is evidently related to the characteristics and the content of potentially reactive phases/components, specifically the high Ca and low Si and Al content, which do not allow the formation of 3-dimensional Si-Al networks, which typically provide the strength in alkali-activated materials.

3.3. Mechanical activation of oil shale CFBC fly ash

3.3.1. Activation of CFBC fly ash and the properties of ash paste

CFBC technology, which has gradually been replacing PC technology worldwide already since the 1990s, is more energy-efficient with lower SO_2 and NO_x emissions (Anthony, 1995; Koornneef et al., 2007; Yue et al., 2017). CFBC allows for efficient firing of low quality Ca and S rich fuels, but the variability of fuels' chemical and phase composition, as well as their lower pozzolanic activity and high content of free CaO and SO_3, has limited the broader use of CFBC ash in cement and concrete composition (Anthony, 1995; Chen et al., 2017; Giergiczny, 2019; Glinicki et al., 2019; Golek, 2019; Hlavacek et al., 2018; Ohenoja et al., 2019; Siler et al., 2015).

The properties of CFBC ash can be improved, for example, by blending, classification-separation, chemical passivation, thermal beneficiation (Robl, 2017) and the mechanical activation of fly ash by grinding. The latter is one of the simplest measures increasing its surface area, thereby increasing ash reactivity (Fernandez-Jimenez et al., 2019; Hela and Orsakova, 2013; Kumar and Kumar, 2011).

Mechanical activation without changing the chemical composition of materials is commonly used to improve their bulk and surface reactivity by increasing the particles' surface area and altering their surface and crystal structure properties, which can collectively enhance their hydration and dissolution rates (Kumar and Kumar, 2011; Kumar et al., 2017). Marjanovic et al. (2014) have shown a more than tenfold increase in the compressive strengths of geopolymers made of mechanically activated thermal power plant fly ash, compared to a geopolymer made of raw ash precursor. Similarly, the cement-free activation of Ca-rich fly ash, combining mechanical activation and blending with

silica fume and flue gas desulfurization gypsum as a grinding aid, and/or polycarboxilate ether based plasticiser additive and NaOH alkali activation, was reported to yield ca. 35% increase in compressive strength, reaching a maximum of 46 MPa in 28 days, compared to blends made without mechanical activation (Sadique et al., 2013).

The mechanical activation of oil shale Ca-rich CFBC TA shows nearly an order of magnitude improvement in the compressive strength of ash pastes made with plain water, both in terms of final strength (60 MPa after 90 days) as well as early strength development (30 MPa in 7 days), without using any chemical activation or blending (Fig. 7) (Paaver et al., 2021—PAPER III).

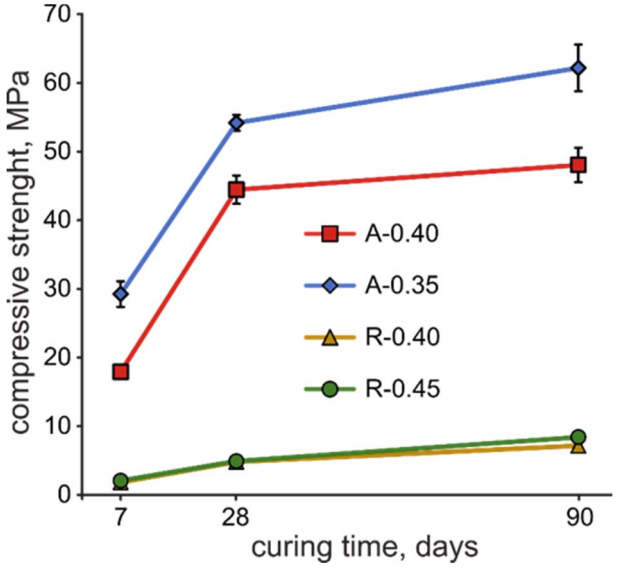

Figure 7. Compressive strength of raw fly ash pastes and pastes made with ash grinded for 4 min, mixed at different water/ash ratios (0.35, 0.4, and 0.45) and cured for 7, 28, and 90 days.

It is peculiar that the uniaxial compressive strengths of pastes made with raw ash were between 1 to 2.4 MPa after 7 days of curing, while mechanically activating the ash for only 2 minutes in a planetary ball mill improved the compressive strength of ash-water paste by order of magnitude, reaching 20.3 MPa in the mixture with a water/ash ratio of 0.35 after seven days (Fig. 8).

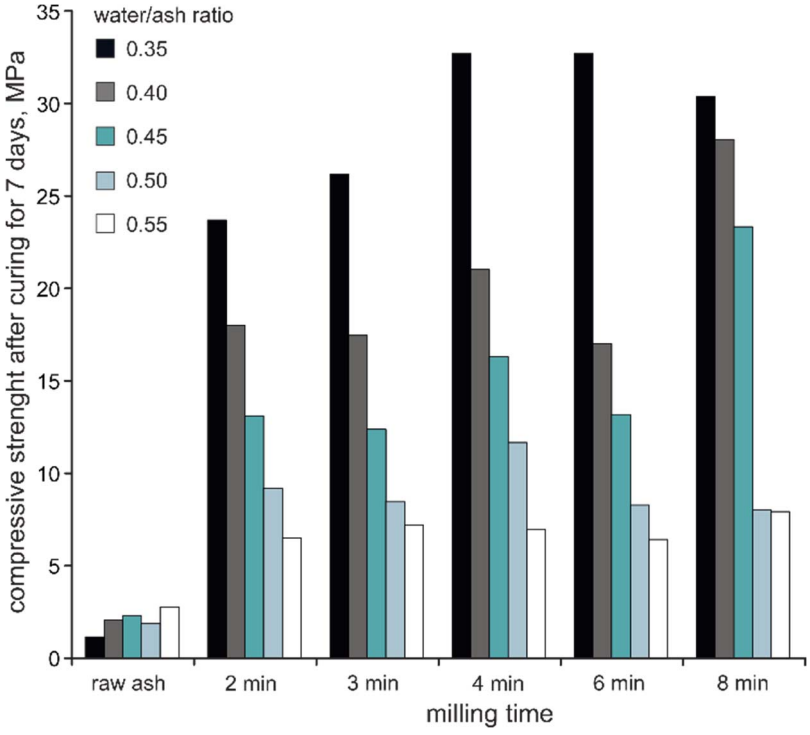

Figure 8. Uniaxial compressive strength of ash pastes made with raw ash and pastes made with ash milled for 2, 3, 4, 6, and 8 min, mixed at different water/ash ratios (0.35, 0.4, 0.45, 0.5, and 0.55) and cured for 7 days. (Paaver et al., 2021—PAPER III).

Pastes made with the same water/ash ratio but different grinding times achieved the compressive strengths of 22.4, 29.2, 28.1 and 25.0 MPa with 3, 4, 6 and 8 minutes grinding time, respectively. This means that even a relatively short period of milling significantly improves the paste's strength (Fig. 8). Although the compressive strength of activated ash pastes is sensitive to water/ash ratio, with values dropping exponentially when water content increases, even at the highest water/ash ratio (0.55) the compressive strength values of mechanically activated ash pastes are at least twice as high as those of raw ash pastes (Fig. 8).

During the grinding of fly ash particles are broken up, increasing the fineness and specific surface area of ash, but also generating crystalline defects, leading to an increase in the amorphous phase and enhancing the overall reactivity of ash (Kumar et al., 2017). The raw oil shale CBC TA is characterized by a nearly normal grain size distribution, with the mean grain size of 43 μm (Fig. 9) and particle shapes dominated by irregular-flaky porous lumps and aggregates of 50–80 μm, as well as spherical cenospheres of 1 to 20 μm (rarely up to 50–100 μm) in diameter (Fig. 10). Grinding in a planetary ball mill causes the breaking up of easily friable large lumps into sub-μm fine particles. However, while large-sized lumps are broken up into irregular pieces (Fig 10), most of the small (<10 μm) cenospheres retain their integrity. In overall the grain size distribution shifts in

favour of finer particles. The effectiveness of milling started to decrease when milling times exceeded 6 minutes due to particle agglomeration in ground ash material (Tole et al., 2019). At the same time, the specific surface area of ash increased from 2.5 $m^2 g^{-1}$ in raw ash to 4.7 $m^2 g^{-1}$ and 4.9 $m^2 g^{-1}$ after 4 min and 8 min, respectively (Fig. 9b).

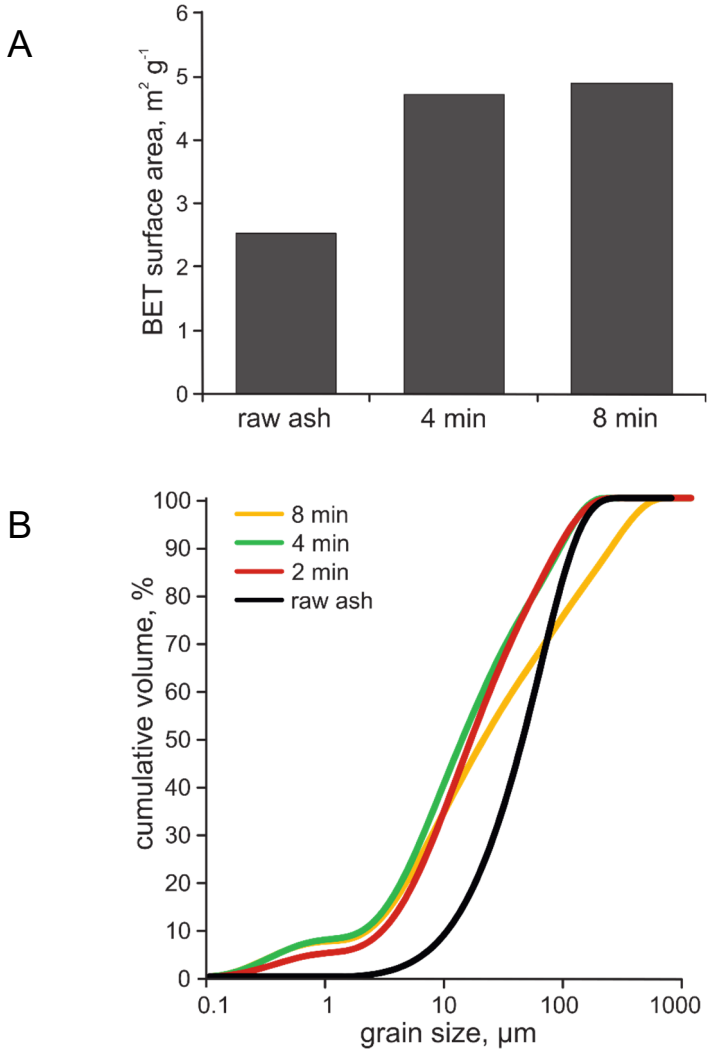

Figure 9. Specific surface area of raw and mechanically activated ash milled for 4 and 8 min (A) and cumulative grain size distribution of raw and activated ash (milling for 2, 4, and 8 min) (B) (Paaver et al., 2021—PAPER III).

Interestingly, although the increase in compressive strength is nearly sixfold when compared to the paste made with raw ash, the increase in specific surface area is only twofold after milling. This suggests that the effect of short mechanical activation on CFBC fly ashes resides not in the fine milling *per se*, but rather in the fragmentation of large irregular flaky porous lumps and aggregates into sub-µm-sized constituents that increases the reactivity and makes a compact structure of the paste.

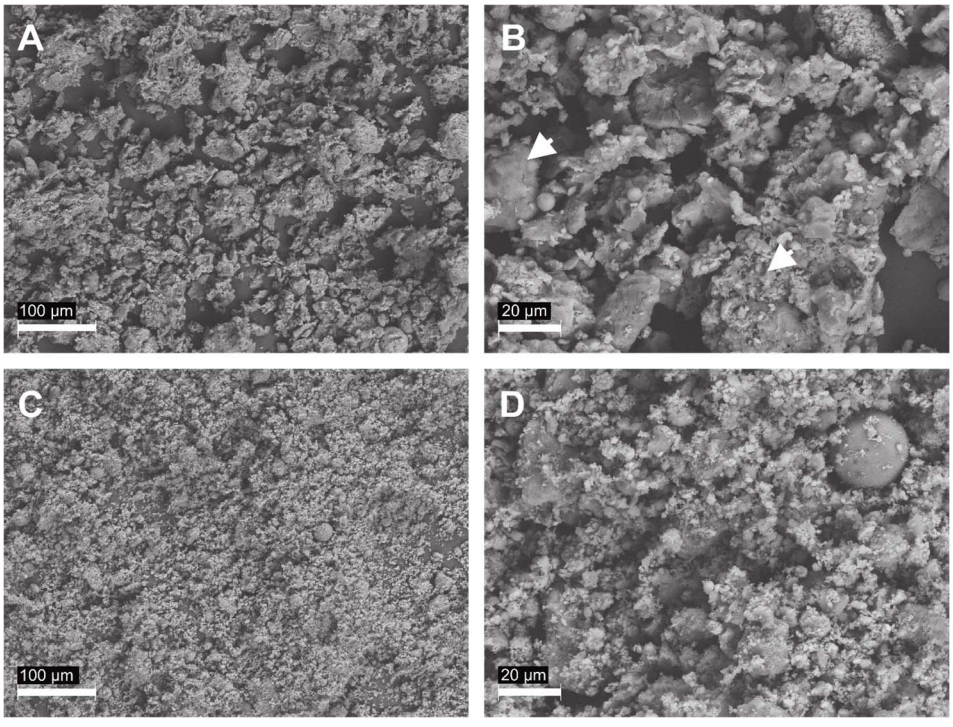

Figure 10. SEM backscattered electron images of raw ash (A,B) and ash milled for 8 min (C,D). (Paaver et al., 2021—PAPER III).

The agglomeration of ash particles and the significant reduction in their fineness is a particular feature of CFBC boilers, where SO_2 is effectively removed from the circulating boiler system by flue gas reaction, with calcined limestone forming relatively large particles composed of dense $CaSO_4$ shells on unreacted CaO cores (Anthony and Granatstein, 2001; Wu and Anthony, 2011). The breaking of hard and impermeable anhydrite shells also has an immediate effect on the anhydrite dissolution rate, causing it to disappear from mechanically activated CFBC fly ash already after 7 days of curing, whereas in pastes made with raw ash anhydrite remains detectable for 90 days (Fig. 11).

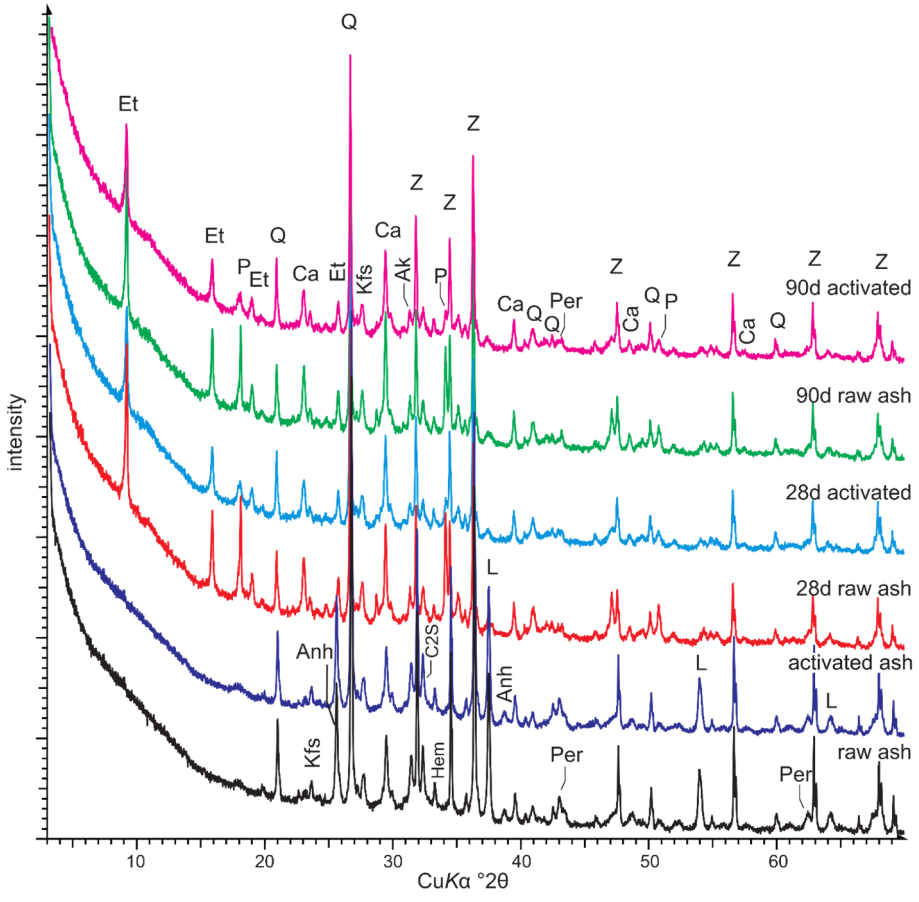

Figure 11. Representative XRD patterns of raw ash, ash mechanically activated for 4 min and activated ash pastes after 28 and 90 days of curing. Legend for major peaks: Ak—akermanite; Anh—anhydrite; Ca—calcite; C2S—belite; Et—ettringite; Hem—hematite; Kfs—K-feldspar; L—lime; P—portlandite; Per—periclase; Q—quartz; Z—zinc oxide. ZnO spike was added to samples to estimate the amorphous phase content (Paaver et al., 2021—PAPER III).

The cementitious properties of both raw and activated ash pastes are evidently most affected by the formation of abundant crystalline ettringite ($Ca_6Al_2(OH)_{12}(SO_4)_3 \cdot 26H_2O$). In addition, the dissolution of Ca- and Ca-Mg silicates, i.e. belite and merwinite/akermanite, continued during the full course of the hydration period, possibly producing a heterogeneous C-(A)-S-H gel-like phase with additional crystalline portlandite $Ca(OH)_2$ formed by the hydration of lime (Fig. 11).

The formation of the secondary hydrous Ca-Al sulphate phase—ettringite—chronologically follows the slacking of lime, possibly occurring in parallel with anhydrite dissolution. The content of ettringite, assessed semiquantitatively by means of the XRD method, reaches ca. 15–17 wt% already after 7 days of curing,

remained nearly at the same level for the 90-day curing period both in raw and activated ash pastes. At the same time, the share of amorphous phase increased to a maximum of 45 wt% in activated ash pastes after 28 days of curing, decreasing to about 32 wt% after 90 days.

The phase composition of ash pastes is further confirmed by ATR-FT-IR spectra, indicating portlandite formation and particularly the dissolution of anhydrite in hydrated pastes, as evidenced by the absence of characteristic anhydrite bands near 595, 611 and 680 cm^{-1}. Instead, a broad and intense band appears at about 1090 cm^{-1}, constituting a combination of Si-O stretching vibrations from the silicate phases associated with Q^3 silicon sites (Rees et al., 2007) and S-O vibrations in SO_4^{2-} arising from different sulphate minerals, such as ettringite, as also seen in the XRD analysis. Interestingly, a broad band at 973 cm^{-1} in raw ash, resulting from the vibrations of Si-O-Si, grows in intensity and sharpens in pastes made with mechanically activated ash (see Fig. 8 in Paaver et al., 2021—PAPER III). The position of this band shifts to lower wavenumbers at 958–960 cm^{-1} in all pastes after 28 and 90 days of curing, indicating that the initially formed structures possibly deformed in time, resulting in the replacement of bridging oxygen atoms in the initial alumina-silicate phase with two non-bridging oxygen atoms with a negative charge. It could also indicate that Al is possibly introduced into the silicate network (Hajimohammadi et al., 2008). Furthermore, the TG analysis showing characteristic mass changes corresponding to ettringite, portlandite and carbonate decomposition (see Fig. 9 in Paaver et al., 2021—PAPER III) also shows mass loss without clear peaks between the temperatures 125 and 275°C. This could be tentatively attributed to C-S-H or other possible X-ray amorphous phases, even though the identification of C-S-H-type phases is complicated in TG analysis due to the multitude and overlapping of phases in ash pastes (Scrivener et al., 2018b; Zhang and Ye, 2012).

Overall, Ca-rich CFBC fly ash behaves similarly to calcium sulfoaluminate (CSA) cement, which is considered as one of the low-CO_2 alternatives to OPC (Ben Haha et al., 2019). In CSA hydration, strength development is provided by the hydration of ye'elimite ($Ca_4(AlO_2)_6SO_3$) in the presence of gypsum ($CaSO_4$ $2H_2O$), producing ettringite and nanocrystalline $Al(OH)_3$, and depending on cement composition, other phases, such as monosulfate, C-S-H phase, strätlingite, or hydrogarnet (Martin et al., 2017; Telesca et al., 2014; Winnefeld and Lothenbach, 2010).

In Ca- and S-rich CFBC ashes, ettringite is formed by the reaction of anhydrite/gypsum and Al-bearing phases. The availability of Ca-sulphate is typically regarded as limiting the ettringite formation in hydrated CFBC ashes (Bernardo et al., 2004). However, Ca-rich CFBC ash is low in reactive silica and aluminium, but it is rich in Ca-sulfate and able to precipitate with ettringite concurrent gypsum (Liira et al., 2009a; Pihu et al., 2012). Hence, it is the presence and availability of dissolved Al species, rather than sulphate, which limits ettringite formation in Ca-rich CFBC ash. This is further supported by the absence of excess Al-hydroxide precipitation, characteristic to CSA cements, even though Al-hydroxide precipitation is also suppressed by the presence of

$Ca(OH)_2$ (Ben Haha et al., 2019; Winnefeld and Lothenbach, 2010), which is abundant in hydrated Ca-rich CFBC fly ashes.

The main readily available Al sources in Ca-rich oil shale CFBC ashes are amorphous Ca-Si-Al-(K) cenospheres and/or residual dehydroxylated aluminosilicate clays. On one hand, $Al(OH)_4^-$ ions' diffusion from Al-bearing phases into the pore space is inhibited in the presence of lime and gypsum in the early stages of hydration (Min and Mingshu, 1994). On the other hand, due to retarded Al mobility, the interfaces of Al-phases become supersaturated with respect to ettringite, causing an explosive formation of small nano-crystallites at a high nucleation rate (Liira et al., 2009a). This, in turn, provides the early strength in hardening pastes, whereas ettringite recrystallizes into a larger and well-crystalline form with progressing hydration, providing the concurrent development of C-(A)-S-H gel-like phase at the expense of the dissolution of glassy cenospheres and the firm bonding of their fragments in Ca-rich CFBC ash pastes.

The effect of fly ash grinding, which causes the paramount distinction between the compressive strength of the raw and activated ash pastes, is concerned with the final compactness of paste microstructure (Fig. 12). In pastes made with raw ash, intact aggregates form a highly porous microstructure, bridged only at tangential grain contacts by ettringite, calcite and portlandite precipitates. However, in pastes made with activated fly ash, the entire space between unreacted particles is filled with dense sub-μm fibrous aggregate ettringite webs and possibly a (semi)-amorphous calcium-silica-hydrate (C-S-H) phase providing the high compactness of the paste (Fig. 12). The dynamics of the estimated amorphous phase content in pastes suggests that in the first stages of hydration, the most reactive phases form an X-ray amorphous gel-like phase, the content of which increases over 28 days of curing, but shows a decrease after 90 days, indicating the recrystallization of amorphous mass into stable crystalline phases, which in this case means calcite, hydrocalumite and ettringite.

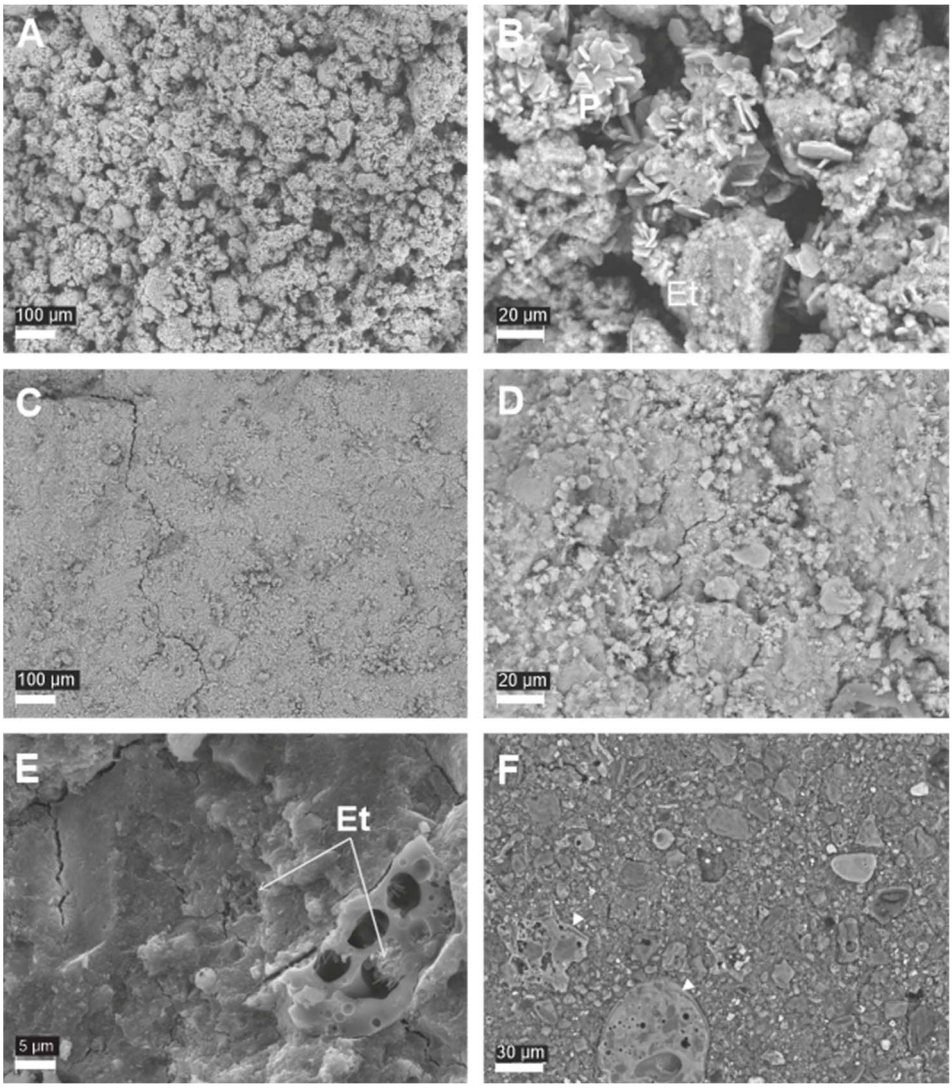

Figure 12. SEM backscattered electron images of pastes made with raw ash (A, B) and mechanically activated ash after 90 days of curing (C, G). Et—ettringite (Paaver et al., 2021—PAPER III).

3.3.2. Design of high volume activated CFBC fly ash and ordinary Portland cement mixtures

The production of ordinary Portland cement (OPC) emits a large fraction, i.e. about 8%, of manmade greenhouse emissions (Gartner and Hirao, 2015). Hence, finding alternative raw materials, minimizing the carbon dioxide emissions from binders production, developing substitute and/or supplementary cementitious materials and designing alternative low-carbon binders have become the priority

of the cement industry (Hanein et al., 2018). Paaver et al. (2021—PAPER III) have shown that mechanically activated high calcium fly ashes from circulating fluidized bed combustion (CFBC) boilers with a high content of free CaO, Ca-sulphate with belite and alumosilicate minerals (and Ca-Si-Al-rich glassy phase) behave similarly to Ca-sulfoaluminate (CSA) cements, yielding comparable compressive strengths without any need for calcination, chemical activation or blending with other types of binders while, similarly to CSA cement, the cementitious properties of activated CFBC ash are controlled by the formation of crystalline ettringite and a heterogeneous C-(A)-S-H gel-like phase (Paaver et al., 2021—PAPER III).

Calcium sulfoaluminate (CSA) and Ca-sulfoaluminate-belite cements (CSA-C2S) are increasingly becoming known as sustainable, less CO_2-intensive alternatives to ordinary Portland cement (Ben Haha et al., 2019; Chaunsali and Mondal, 2015; Glasser and Zhang, 2001; Hargis et al., 2014; Juenger et al., 2019; Juenger et al., 2011). However, CSA cements are typically produced by the calcination of limestone and Al-rich raw materials (bauxite, Al-clay, fly ash, "red mud") at ca. 1250°C, and addition of gypsum or phosphogypsum (Chen and Juenger, 2012; Hertel et al., 2021; Julphunthong and Joyklad, 2019; Rungchet et al., 2016; Shen et al., 2015; Zibret et al., 2021; Telesca et al., 2016; Telesca et al., 2020). The mechanically activated oil shale CFBC ash, however, does not require additional calcination nor chemical activation. Hence, mechanically activated Ca- and sulphate rich CFBC fly ashes constitute alternative CSA-type cementitious materials that can potentially replace OPC, meaning that mechanical activation would significantly widen the reuse and applicability of these materials in different fields of construction and soil mass-stabilization.

OPC pastes with activated CFBC ash, where 50% of OPC was substituted with activated ash resulted in nearly the same average uniaxial compressive strength as that of a pure OPC compound, reaching the values 40 MPa and 43 MPa after 7 days of hydration, and 54 MPa and 58 MPa after 28 days (Fig 13b; Paaver et al, in preparation—PAPER IV). At the same time, the uniaxial compressive strength of raw CFBC paste made with OPC decreases nearly linearly from on average 58.2 MPa in a pure OPC compound to ca. 9 MPa in 100% raw ash after 28 days of curing. Although pastes made with <50% raw FA substitution for OPC show a slight increase in compressive strength values after 7 days of hydration, suggesting that the activation of the ash-OPC system and ash hydration contribute to the overall strength development at the early stages, then raw CFBC ash seems to behave rather as an inert component in the long term (Fig 13a).

Pure activated CFBC ash and paste made with 75% OPC replacement also showed significantly higher compressive strength values than those of raw CFBC ash pastes, reaching ~36 and 42 MPa after 28 days of curing, respectively (Fig. 13b). Similarly, after 28 days of curing mortars made with sand and activated CFBC ash yield an average compressive strength of 37.6, 34.7 and 17.6 MPa for 25%, 50% and 75% sand content, respectively, whereas their compressive strength reaches 10 MPa or more for all mortar mixtures already after 7 days (Fig. 14a; Paaver et al, in preparation—PAPER IV).

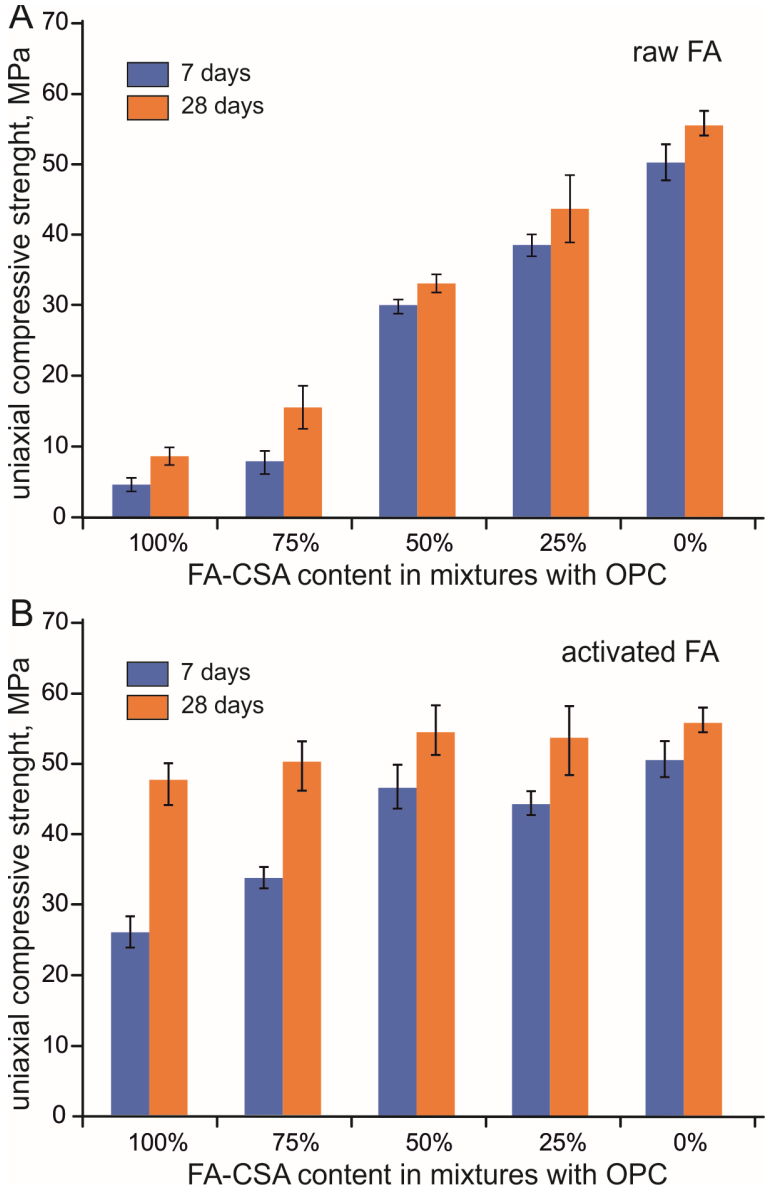

Figure 13. Average uniaxial compressive strength of OPC mixture pastes made with raw (A) and mechanically activated (B) fly ash after 7 and 28 days of hydration (Paaver et al., in preparation—PAPER IV).

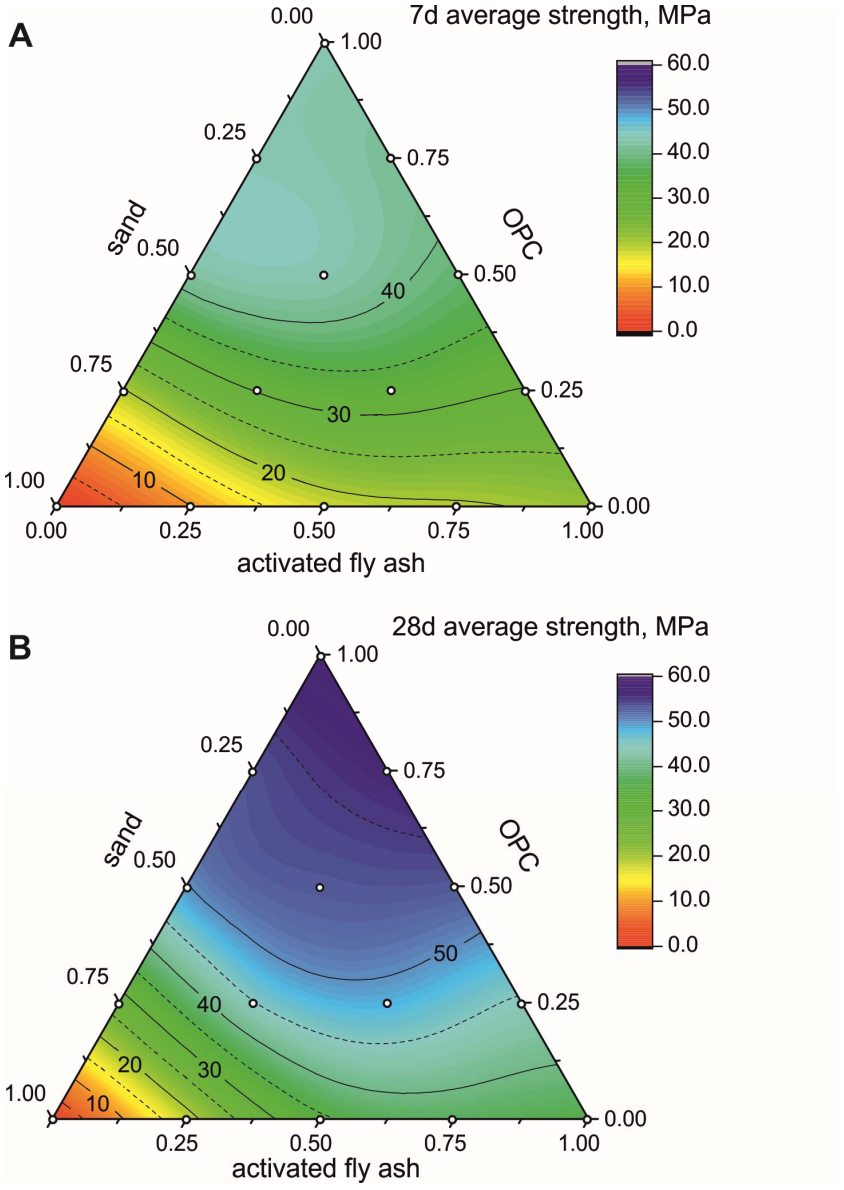

Figure 14. Uniaxial compressive strength of OPC-FA-CSA and sand mixtures after 7 (A) and 28 days (B) of hydration. Isolines show the uniaxial compressive strength in MPa. (Paaver et al., in preparation—PAPER IV)

It is noteworthy that activated CFBC ash and mortars made with 25% and 50% of normalized sand yield nearly the same compressive strength value (36–38 MPa) after 28 days of curing. Mortars where OPC is replaced with activated CFBC ash reach compressive strength values >30 MPa in 7 days and >45 MPa after 28 days. For example, the mortar with 50/25/25 ratio of sand, OPC and FA-CSA, respectively, yielded an average uniaxial compressive strength value of 30.3 MPa after 7 days and 44.7 MPa after 28 days of curing (Fig. 14b; Paaver et al, in preparation—PAPER IV).

Notably, the reduction in the compressive strength of the mortars made with a 50% FA-CSA replacement for OPC, when compared to the equivalent 50/50 mortar made with only OPC and sand, is only approximately 10%, suggesting that FA-CSA can be successfully used for high-volume OPC replacement. In comparison, the reported reductions in the compressive strength of mortars made with FA replacement for OPC are typically larger than 40% for mixtures with replacement rates higher than 50% (Nwankwo et al., 2020; Shaikh et al., 2014; Supit et al., 2014).

It is interesting that the average compressive strength of the 50/50 OPC-activated CFBC ash paste (~40 MPa) is somewhat higher than 75/25 OPC-activated CFBC ash paste (~38 MPa) after 7 days of hydration, indicating that adding activated CFBC ash improves the development of early strength in mixtures with OPC (Paaver et al., in preparation—PAPER IV). One of the major drawbacks that has been highlighted for high-volume OPC replacement with FA is its retarded strength development at the early stages of hydration (Giergiczny, 2019; Nwankwo et al., 2020). During the first weeks of hydration, fly ash typically acts like an inert filler that may have some beneficial properties providing denser packing and seeding effects, but that does not contribute much to the strength development (Nwankwo et al., 2020).

The pozzolanic reactions between CFBC ash and alkaline environment controlled by Ca-hydroxide, which produces the C-(A)-S-H gels providing cementitious properties, are delayed because of the slow build-up of the alkalinity needed for ash particles' dissolution in the pore solution. This lasts until pH reaches 12 as silica hydration is significantly advanced in solutions with pH > 11.8 (Bellmann and Stark, 2009). This propensity of slow hydration in fly ash-OPC pastes is characteristic of Class F fly ashes rich in silica and aluminium (Nwankwo et al., 2020). However, in CFBC ashes, which are mainly classified as Class C fly ash enriched with Ca and sulphate, early strength is produced by the rapid precipitation of ettringite rather than C-S-H gel formation. Hence, CFBC ashes are devoid of slow reactivity, providing excellent compressive strength already during the first days of the hydration. At later stages, when pozzolanic reactions are activated by the raising pH in pore-solution, it is possible that the formation of C-(A)-S-H gel-like masses contribute to strength development at the later stages (Paaver et al., 2021—PAPER III) and that over time such pastes/mortars achieve strengths comparable to mixtures with OPC. Paaver et al. (2021—PAPER III) have shown in agreement with other similar studies (Giergiczny, 2005; Marjanovic et al., 2014; Scrivener et al., 2018a) that the high

compressive strength of activated CFBC ash pastes is associated with the development of a more compact microstructure of the mechanically activated fly ash pastes and mortars improving the bonding between paste particles and aggregates. The more compact structure of activated FA pastes and mortars is evident from the scanning electron imaging of these pastes and mortars (see Figure 7 in Paaver et al., in preparation—PAPER IV), showing the progressive filling of pore space with dense ettringite meshes and, possibly, C-(A)-S-H gel-like masses.

4. CONCLUSIONS

The aim of this thesis was to characterize the cementitious properties, alkali activation and mechanical activation of circulated fluidized bed combustion (CFBC) and solid heat carrier (SHC) ashes from Estonian power plants and oil retorts, in order to evaluate their potential use for the development of alternative binder systems using alkali activation and mechanical activation.

Fly-ash-based binders are viable alternatives for CO_2-extensive cement clinker systems. While low-calcium fly ashes rich in siliceous glass are primarily used in blends with ordinary cement or for production of alkali-activated binders, the use of high-calcium fly ashes, particularly those produced in circulating fluidized bed combustion boilers with high content of free CaO and $CaSO_4$, has been hindered, mainly due to their variable composition and poor cementitious properties. This study shows, however, that Ca- and S-rich CFBC ashes can be successfully used as alternative binders after simple mechanical activation.

The main results of the study are:

1) The ash from CFBC boilers and Enefit280 retorts is only partly decarbonated, containing significantly less free lime and secondary Ca-Mg silicates with pozzolanic properties than ash from older, decommissioned pulverized combustion (PC) boilers. Except for the fly ash collected from the electrostatic filters at Auvere power plant, all CFBC ash types show low self-cementitious properties, requiring physical-chemical or thermal pre-treatments and/or blending in order to be used in construction applications.
2) Alkali activation of Estonian Ca-rich oil shale solid waste shows that even though polymerization reactions occur by forming polymeric C-(A)-S-H type structures, the overall geopolymeric potential of oil shale ashes is low. Compared to other industrial waste materials used for alkali activation and geopolymer production, Ca-rich oil shale fly ash is considerably lower in reactive Si and Al, which are required for building Si-Al polymeric networks. In addition, the development of dense microfracturing and the strong dry shrinkage of alkali-activated oil shale fly ash causes significant weakening in the material in the long term.
3) Even a short period of mechanical activation of the Ca-rich oil shale CFBC fly ash yields a nearly tenfold improvement in the compressive strength of hydrated fly ash pastes, topping at 60 MPa after 90 days without any chemical activation or blending. Mechanical activation facilitated the fragmentation of large irregular flaky porous lumps and aggregates characteristic to CFBC ashes, improving the reactivity by creating finer grain size, larger surface area and disintegration of compact $CaSO_4$ shells on unreacted CaO cores.
4) The cementitious properties of Ca-rich CFBC ash are mainly controlled by the formation of crystalline ettringite ($Ca_6Al_2(OH)_{12}(SO_4)_3 \cdot 26H_2O$), and possibly a heterogeneous C-(A)-S-H gel-like phase. In mechanically activated

fly ash pastes, the enhancement of mechanical strength is achieved by a significantly more compact microstructure, where pore space between unreacted particles is completely filled with dense webs of ettringite crystallites, calcite from portlandite carbonation and a gel-like Ca-Al-Si phase.

5) Phase development in activated Ca-rich CFBC fly ash is similar to that in calcium sulfoaluminate (CSA) cements, where hydration of ye'elimite in the presence of gypsum produces ettringite and nanocrystalline Al-hydroxide. Ettringite forms in Ca- and sulfate-rich CFBC ashes by the reaction of anhydrite and Al-bearing phases (glass, clay minerals, feldspars), possibly being limited by the availability of reactive Al phases.
6) In pastes and mortars with ordinary Portland cement (OPC), raw Ca- and S-rich oil shale CFBC ash acts as an inert filler. Mechanically activated fly ash, however, performs as an active binder, allowing a high volume of OPC replacement. The pastes and mortars where 50% of OPC has been replaced with mechanically activated fly ash yield nearly the same compressive strength values as in pastes/mortars with only OPC, the reduction in strength being less than 10%.
7) Substituting OPC with activated CFBC ash improves the development of early strength in the mixtures by the formation of dense ettringite crystallite meshes. In the later stages, strength development is facilitated by pozzolanic reactions triggered by the elevated pH of the pore solution, leading to the formation of C-(A)-S-H gel-like masses. This suggests that mechanically activated Ca-rich CFBC fly ashes can be successfully used as an alternative Ca-sulfoaluminate cement type binder.

Our findings suggest that while untreated and alkali-activated oil shale ashes generally tend to show poor cementing properties, mechanically activated ashes potentially represent a viable material for full or partial replacement of the ordinary Portland cement. Further studies should evaluate long term behavior of the activated CFBC systems and test the durability of the material in real world conditions (freeze-thaw cycles, heat resistance, leaching, etc).

REFERENCES

Anthony, E.J., 1995. Fluidized-Bed Combustion of Alternative Solid Fuels—Status, Successes and Problems of the Technology. Progress in Energy and Combustion Science, 21(3): 239–268.

Anthony, E.J. and Granatstein, D.L., 2001. Sulfation phenomena in fluidized bed combustion systems. Progress in Energy and Combustion Science, 27(2): 215–236.

Arro, H., Pihu, T., Prikk, A., Rootamm, R. and Konist, A., 2009. Comparison of Ash from PF and CFB Boilers and Behaviour of Ash in Ash Fields. In: G. Yue, H. Zhang, C. Zhao and Z. Luo (Editors), Proceedings of the 20th International Conference on Fluidized Bed Combustion. Springer.

Aughenbaugh, K.L., Williamson, T. and Juenger, M.C.G., 2015. Critical evaluation of strength prediction methods for alkali-activated fly ash. Materials and Structures, 48(3): 607–620.

Bauert, H. and Kattai, V., 1997. Kukersite oil shale. In: A. Raukas and A. Teedumäe (Editors), Geology and mineral resources of Estonia. Estonian Academy Publishers, Tallinn, pp. 313–327.

Bellmann, F. and Stark, J., 2009. Activation of blast furnace slag by a new method. Cement and Concrete Research, 39(8): 644–650.

Ben Haha, M., Winnefeld, F. and Pisch, A., 2019. Advances in understanding ye'elimite-rich cements. Cement and Concrete Research, 123.

Berber, H., Tamm, K., Leinus, M.L., Kuusik, R., Tonsuaadu, K., Paaver, P. and Uibu, M., 2019. Accelerated carbonation technology granulation of industrial waste: Effects of mixture composition on product properties. Waste Management & Research.

Berber, H., Tamm, K., Leinus, M.L., Kuusik, R., Tonsuaadu, K., Paaver, P. and Uibu, M., 2020. Accelerated carbonation technology granulation of industrial waste: Effects of mixture composition on product properties. Waste Management & Research, 38(2): 142–155.

Bernardo, G., Telesca, A., Valenti, G.L. and Montagnaro, F., 2004. Role of ettringite in the reuse of hydrated fly ash from fluidized-bed combustion as a sulfur sorbent: A hydration study. Industrial & Engineering Chemistry Research, 43(15): 4054–4059.

Bityukova, L., Mõtlep, R. and Kirsimäe, K., 2010. Composition of Oil Shale Ashes from Pulverized Firing and Circulating Fluidized-Bed Boiler in Narva Thermal Power Plants, Estonia. Oil Shale, 27(4): 339–353.

Buchwald, A., Dombrowski, K. and Weil, M., 2005. The influence of calcium content on the perfomance of geopolymeric binder especially the resistance against acids, 4th International Conference on Geopolymers, St. Quentin, France, pp. 35–39.

Chaunsali, P. and Mondal, P., 2015. Influence of Calcium Sulfoaluminate (CSA) Cement Content on Expansion and Hydration Behavior of Various Ordinary Portland Cement-CSA Blends. Journal of the American Ceramic Society, 98(8): 2617–2624.

Chen, I.A. and Juenger, M.C.G., 2012. Incorporation of coal combustion residuals into calcium sulfoaluminate-belite cement clinkers. Cement & Concrete Composites, 34(8): 893–902.

Chen, X.M., Gao, J.M., Yan, Y. and Liu, Y.Z., 2017. Investigation of expansion properties of cement paste with circulating fluidized bed fly ash. Construction and Building Materials, 157: 1154–1162.

Davidovits, J., 2011. Geopolymer Chemistry and Applications. Institut Géopolymère, Saint-Quentin.

Duxson, P., Fernandez-Jimenez, A., Provis, J.L., Lukey, G.C., Palomo, A. and van Deventer, J.S.J., 2007. Geopolymer technology: the current state of the art. Journal of Materials Science, 42(9): 2917–2933.

Duxson, P. and Provis, J.L., 2008. Designing Precursors for Geopolymer Cements. Journal of the American Ceramic Society, 91(12): 3864–3869.

Fernandez-Jimenez, A., Garcia-Lodeiro, I., Maltseva, O. and Palomo, A., 2019. Mechanical-Chemical Activation of Coal Fly Ashes: An Effective Way for Recycling and Make Cementitious Materials. Frontiers in Materials, 6.

Gartner, E. and Hirao, H., 2015. A review of alternative approaches to the reduction of CO2 emissions associated with the manufacture of the binder phase in concrete. Cement and Concrete Research, 78: 126–142.

Giergiczny, Z., 2005. Effect of fly ash from different sources on the properties of hardened cement composites. Silicates Industriels, 70(3–4): 35–40.

Giergiczny, Z., 2019. Fly ash and slag. Cement and Concrete Research, 124.

Glasser, F.P. and Zhang, L., 2001. High-performance cement matrices based on calcium sulfoaluminate-belite compositions. Cement and Concrete Research, 31(12): 1881–1886.

Glinicki, M.A., Jozwiak-Niedzwiedzka, D. and Dabrowski, M., 2019. The Influence of Fluidized Bed Combustion Fly Ash on the Phase Composition and Microstructure of Cement Paste. Materials, 12(17).

Golek, L., 2019. Glass powder and high-calcium fly ash based binders—Long term examinations. Journal of Cleaner Production, 220: 493–506.

Gosh, S.K. and Kumar, V. (Editors), 2020. Circular Economy and Fly Ash Management. Springer, Singapore, Singapore, 160 pp.

Guo, X.L., Shi, H.S., Chen, L.M. and Dick, W.A., 2010a. Alkali-activated complex binders from class C fly ash and Ca-containing admixtures. Journal of Hazardous Materials, 173(1–3): 480–486.

Guo, X.L., Shi, H.S. and Dick, W.A., 2010b. Compressive strength and microstructural characteristics of class C fly ash geopolymer. Cement & Concrete Composites, 32(2): 142–147.

Hajimohammadi, A., Provis, J.L. and van Deventer, J.S.J., 2008. One-Part Geopolymer Mixes from Geothermal Silica and Sodium Aluminate. Industrial & Engineering Chemistry Research, 47(23): 9396–9405.

Hanein, T., Galvez-Martos, J.L. and Bannerman, M.N., 2018. Carbon footprint of calcium sulfoaluminate clinker production. Journal of Cleaner Production, 172: 2278–2287.

Hargis, C.W., Telesca, A. and Monteiro, P.J.M., 2014. Calcium sulfoaluminate (Ye'elimite) hydration in the presence of gypsum, calcite, and vaterite. Cement and Concrete Research, 65: 15–20.

Hela, R. and Orsakova, D., 2013. The Mechanical Activation of Fly Ash. Concrete and Concrete Structures 2013—6th International Conference, Slovakia, 65: 87–93.

Hertel, T., Van den Bulck, A., Onisei, S., Sivakumar, P.P. and Pontikes, Y., 2021. Boosting the use of bauxite residue (red mud) in cement—Production of an Fe-rich calciumsulfoaluminate-ferrite clinker and characterisation of the hydration. Cement and Concrete Research, 145.

Hlavacek, P., Sulc, R., Smilauer, V., Rossler, C. and Snop, R., 2018. Ternary binder made of CFBC fly ash, conventional fly ash, and calcium hydroxide: Phase and strength evolution. Cement & Concrete Composites, 90: 100–107.

Juenger, M.C.G., Snellings, R. and Bernal, S.A., 2019. Supplementary cementitious materials: New sources, characterization, and performance insights. Cement and Concrete Research, 122: 257–273.

Juenger, M.C.G., Winnefeld, F., Provis, J.L. and Ideker, J.H., 2011. Advances in alternative cementitious binders. Cement and Concrete Research, 41(12): 1232–1243.

Julphunthong, P. and Joyklad, P., 2019. Utilization of Several Industrial Wastes as Raw Material for Calcium Sulfoaluminate Cement. Materials, 12(20).

Kaasik, A., Vohla, C., Motlep, R., Mander, U. and Kirsimae, K., 2008. Hydrated calcareous oil-shale ash as potential filter media for phosphorus removal in constructed wetlands. Water Research, 42(4–5): 1315–1323.

Kasak, K., Motlep, R., Truu, M., Truu, J., Koiv-Vainik, M., Espenberg, M., Paiste, P., Kirsimae, K. and Mander, U., 2016. Hydrated Oil Shale Ash Mitigates Greenhouse Gas Emissions from Horizontal Subsurface Flow Filters for Wastewater Treatment. Water Air and Soil Pollution, 227(9).

Kattai, V., Saadre, T. and Savitski, L., 2000. Estonian oil shale: geology, resources and mining conditions Eesti Geoloogiakeskus, Tallinn, 226 pp.

Kikas, W., Ojaste, K. and Raado, L., 1999. Cause and mode of action of the alkali-silica reaction in concretes made with Estonian Portland oil shale cement. Zkg International, 52(2): 106–111.

Kõiv, M., Liira, M., Mander, U., Mõtlep, R., Vohla, C. and Kirsimäe, K., 2010. Phosphorus removal using Ca-rich hydrated oil shale ash as filter material—The effect of different phosphorus loadings and wastewater compositions. Water Research, 44(18): 5232–5239.

Kõiv, M., Ostonen, I., Vohla, C., Mõtlep, R., Liira, M., Lõhmus, K., Kirsimäe, K. and Mander, U., 2012. Reuse potential of phosphorus-rich filter materials from subsurface flow wastewater treatment filters for forest soil amendment. Hydrobiologia, 692(1): 145–156.

Kõiv, M., Vohla, C., Mõtlep, R., Liira, M., Kirsimäe, K. and Mander, U., 2009. The performance of peat-filled subsurface flow filters treating landfill leachate and municipal wastewater. Ecological Engineering, 35(2): 204–212.

Koornneef, J., Junginger, M. and Faaij, A., 2007. Development of fluidized bed combustion—An overview of trends, performance and cost. Progress in Energy and Combustion Science, 33(1): 19–55.

Kumar, S. and Kumar, R., 2011. Mechanical activation of fly ash: Effect on reaction, structure and properties of resulting geopolymer. Ceramics International, 37(2): 533–541.

Kumar, S., Mucsi, G., Kristaly, F. and Pekker, P., 2017. Mechanical activation of fly ash and its influence on micro and nano-structural behaviour of resulting geopolymers. Advanced Powder Technology, 28(3): 805–813.

Kuusik, R., Turn, L., Trikkel, A. and Uibu, M., 2002a. Carbon dioxide binding in the heterogeneous systems formed at combustion of oil shale. 2. Interactions of system components thermodynamic analysis. Oil Shale, 19(2): 143–160.

Kuusik, R., Uibu, M. and Kirsimae, K., 2005. Characterization of oil shale ashes formed at industrial-scale CFBC boilers. Oil Shale, 22(4): 407–419.

Kuusik, R., Uibu, M., Kirsimäe, K., Mõtlep, R. and Meriste, T., 2012. Open-Air Deposition of Estonian Oil Shale Ash: Formation, State of Art, Problems and Prospects for the Abatement of Environmental Impact. Oil Shale, 29(4): 376–403.

Kuusik, R., Uibu, M., Trikkel, A. and Kaljuvee, T., 2006. Reuse of waste ashes formed at oil shale based power industry in Estonia. Waste Management and the Environment Iii, 92: 111–120.

Kuusik, R., Veskimae, H. and Uibu, M., 2002b. Carbon dioxide binding in the heterogeneous systems formed at combustion of oil shale—3. Transformations in the system suspension of ash-flue gases. Oil Shale, 19(3): 277–288.

L'vov, B.V., 2007. Thermal Decomposition of Solids and Melts. Springer, Dordrecht, Dordrecht, 247 pp.

Leben, K., Mõtlep, R., Konist, A., Pihu, T. and Kirsimäe, K., 2021. Carbon dioxide sequestration in power plant Ca-rich ash waste deposits. Oil Shale, 38(1): 65–88.

Leben, K., Mõtlep, R., Paaver, P., Konist, A., Pihu, T., Paiste, P., Heinmaa, I., Nurk, G., Anthony, E.J. and Kirsimäe, K., 2019. Long-term mineral transformation of Ca-rich oil shale ash waste. Science of the Total Environment, 658: 1404–1415.

Liira, M., Kirsimäe, K., Kuusik, R. and Mõtlep, R., 2009a. Transformation of calcareous oil-shale circulating fluidized-bed combustion boiler ashes under wet conditions. Fuel, 88(4): 712–718.

Liira, M., Koiv, M., Mander, U., Mõtlep, R., Vohla, C. and Kirsimäe, K., 2009b. Active Filtration of Phosphorus on Ca-Rich Hydrated Oil Shale Ash: Does Longer Retention Time Improve the Process? Environmental Science & Technology, 43(10): 3809–3814.

Luukkonen, T., Abdollahnejad, Z., Yliniemi, J., Kinnunen, P. and Illikainen, M., 2018. One-part alkali-activated materials: A review. Cement and Concrete Research, 103: 21–34.

Marjanovic, N., Komljenovic, M., Bascarevic, Z. and Nikolic, V., 2014. Improving reactivity of fly ash and properties of ensuing geopolymers through mechanical activation. Construction and Building Materials, 57: 151–162.

Martin, L.H.J., Winnefeld, F., Tschopp, E., Muller, C.J. and Lothenbach, B., 2017. Influence of fly ash on the hydration of calcium sulfoaluminate cement. Cement and Concrete Research, 95: 152–163.

Mijarsh, M.J.A., Johari, M.A.M. and Ahmad, Z.A., 2015. Effect of delay time and Na2SiO3 concentrations on compressive strength development of geopolymer mortar synthesized from TPOFA. Construction and Building Materials, 86: 64–74.

Min, D. and Mingshu, T., 1994. Formation and Expansion of Ettringite Crystals. Cement and Concrete Research, 24(1): 119–126.

Mõtlep, R., Kirsimäe, K., Talviste, P., Puura, E. and Jürgenson, J., 2007. Mineral composition of Estonian oil shale semi-coke sediments. Oil Shale, 24(3): 405–422.

Mõtlep, R., Sild, T., Puura, E. and Kirsimäe, K., 2010. Composition, diagenetic transformation and alkalinity potential of oil shale ash sediments. Journal of Hazardous Materials, 184(1–3): 567–573.

Nwankwo, C.O., Bamigboye, G.O., Davies, I.E.E. and Michaels, T.A., 2020. High volume Portland cement replacement: A review. Construction and Building Materials, 260.

Ohenoja, K., Korkko, M., Wigren, V., Osterbacka, J. and Illikainen, M., 2019. Increasing the utilization potential of fly ashes from fluidized bed combustion by mechanical treatments. International Journal of Environmental Science and Technology, 16(4): 1839–1846.

Ots, A., 2006. Oil shale fuel combustion. Tallinna Raamatutrükikoda, Tallinn, 833 pp.

Paat, A., 2002. About the mineralogical composition of Estonian oil shale ash. Oil Shale, 19(3): 321–333.

Paat, A. and Traksmaa, R., 2002. Investigation of the mineral composition of Estonian oil-shale ash using X-ray diffractometry. Oil Shale, 19(4): 373–386.

Paaver, P., Järvik, O. and Kirsimäe, K., in preparation. Design of high volume CFBC fly ash based calcium sulfoaluminate type binder in mixtures with ordinary Portland cement. Manuscript submitted to Materials

Paaver, P., Paiste, P. and Kirsimäe, K., 2016. Geopolymeric Potential of the Estonian Oil Shale Solid Residues: Petroter Solid Heat Carrier Retorting Ash. Oil Shale, 33(4): 373–392.

Paaver, P., Paiste, P., Liira, M. and Kirsimäe, K., 2019. Alkali Activation of Estonian Ca-Rich Oil Shale Ashes: A Synthesis. Oil Shale, 36(2): 214–225.

Paaver, P., Paiste, P., Liira, M. and Kirsimäe, K., 2021. Mechanical Activation of the Ca-Rich Circulating Fluidized Bed Combustion Fly Ash: Development of an Alternative Binder System. Minerals, 11(1).

Paaver, P., Paiste, P., Mõtlep, R. and Kirsimäe, K., 2017. Self-Cementing Properties and Alkali Activation of Enefit280 Solid Heat Carrier Retorting Ash. Oil Shale, 34(3): 263–278.

Paiste, P., Külaviir, M., Paaver, P., Heinmaa, I., Vahur, S. and Kirsimäe, K., 2019. Beneficiation of Oil Shale Processing Waste: Secondary Binder Phases in Alkali Activated Composites. Waste and Biomass Valorization, 10(5): 1407–1417.

Paiste, P., Külaviir, M., Paaver, P., Heinmaa, I., Vahur, S. and Kirsimäe, K., 2017. Beneficiation of Oil Shale Processing Waste: Secondary Binder Phases in Alkali Activated Composites. Waste and Biomass Valorization.

Paiste, P., Liira, M., Heinmaa, I., Vahur, S. and Kirsimäe, K., 2016. Alkali activated construction materials: Assessing the alternative use for oil shale processing solid wastes. Construction and Building Materials, 122: 458–464.

Pets, L., Knot, P., Haldna, J., Shvenke, G. and Juga, R., 1985. Trace elements in kukersite oil shale ash of Baltic Power Plant. Oil Shale, 2: 379–390.

Pihu, T., Arro, H., Prikk, A., Rootamm, R., Konist, A., Kirsimae, K., Liira, M. and Motlep, R., 2012. Oil shale CFBC ash cementation properties in ash fields. Fuel, 93(1): 172–180.

Raado, L.M., Hain, T., Liisma, E. and Kuusik, R., 2014a. Composition and Properties of Oil Shale Ash Concrete. Oil Shale, 31(2): 147–160.

Raado, L.M., Kuusik, R., Hain, T., Uibu, M. and Somelar, P., 2014b. Oil Shale Ash Based Stone Formation—Hydration, Hardening Dynamics and Phase Transformations. Oil Shale, 31(1): 91–101.

Raado, L.M., Tuisk, T., Rosenberg, M. and Hain, T., 2011. Durability Behavior of Portland Burnt Oil Shale Cement Concrete. Oil Shale, 28(4): 507–515.

Rees, C.A., Provis, J.L., Lukey, G.C. and van Deventer, J.S.J., 2007. In situ ATR-FTIR study of the early stages of fly ash geopolymer gel formation. Langmuir, 23(17): 9076–9082.

Robl, T., 2017. 8—Ash beneficiation, quality, and standard criteria. In: T. Robl, A. Oberlink and R. Jones (Editors), Coal Combustion Products (CCP's). Woodhead Publishing, pp. 217–224.

Rungchet, A., Chindaprasirt, P., Wansom, S. and Pimraksa, K., 2016. Hydrothermal synthesis of calcium sulfoaluminate-belite cement from industrial waste materials. Journal of Cleaner Production, 115: 273–283.

Sadique, M., Al-Nageim, H., Atherton, W., Seton, L. and Dempster, N., 2013. Mechano-chemical activation of high-Ca fly ash by cement free blending and gypsum aided grinding. Construction and Building Materials, 43: 480–489.

Scrivener, K.L., John, V.M. and Gartner, E.M., 2018a. Eco-efficient cements: Potential economically viable solutions for a low-CO2 cement-based materials industry. Cement and Concrete Research, 114: 2–26.
Scrivener, K.L., Snellings, R. and Lothenbach, B., 2018b. A practical guide to micro-structural analysis of cementitious materials. CRC Press, 540 pp.
Shaikh, F.U.A., Supit, S.W.M. and Sarker, P.K., 2014. A study on the effect of nano silica on compressive strength of high volume fly ash mortars and concretes. Materials & Design, 60: 433–442.
Shen, Y., Qian, J.S., Huang, Y.B. and Yang, D.Y., 2015. Synthesis of belite sulfo-aluminate-ternesite cements with phosphogypsum. Cement & Concrete Composites, 63: 67–75.
Siler, P., Bayer, P., Sehnal, T., Kolarova, I., Opravil, T. and Soukal, F., 2015. Effects of high-temperature fly ash and fluidized bed combustion ash on the hydration of Portland cement. Construction and Building Materials, 78: 181–188.
Supit, S.W.M., Shaikh, F.U.A. and Sarker, P.K., 2014. Effect of ultrafine fly ash on mechanical properties of high volume fly ash mortar. Construction and Building Materials, 51: 278–286.
Zhang, Q. and Ye, G., 2012. Dehydration kinetics of Portland cement paste at high temperature. Journal of Thermal Analysis and Calorimetry, 110(1): 153–158.
Zhang, Z.H., Provis, J.L., Reid, A. and Wang, H., 2014a. Fly ash-based geopolymers: The relationship between composition, pore structure and efflorescence. Cement and Concrete Research, 64: 30–41.
Zhang, Z.H., Wang, H., Zhu, Y.C., Reid, A., Provis, J.L. and Bullen, F., 2014b. Using fly ash to partially substitute metakaolin in geopolymer synthesis. Applied Clay Science, 88–89: 194–201.
Zibret, G., Teran, K., Zibret, L., Ster, K. and Dolenec, S., 2021. Building of the Al-containing Secondary Raw Materials Registry for the Production of Low CO2 Mineral Binders in South-Eastern European Region. Sustainability, 13(3).
Tamm, K., Viires, R., Kuusik, R. and Uibu, M., 2017. Calcium Extraction from Estonian Industrial Wastes Based on Ammonium Solvents. Energy and Sustainability Viii, 224: 465–476.
Telesca, A., Marroccoli, M., Pace, M.L., Tomasulo, M., Valenti, G.L. and Monteiro, P.J.M., 2014. A hydration study of various calcium sulfoaluminate cements. Cement & Concrete Composites, 53: 224–232.
Telesca, A., Marroccoli, M., Tomasulo, M., Valenti, G.L., Dieter, H. and Montagnaro, F., 2016. Low-CO2 Cements from Fluidized Bed Process Wastes and Other Industrial By-Products. Combustion Science and Technology, 188(4–5): 492–503.
Telesca, A., Matschei, T. and Marroccoli, M., 2020. Study of Eco-Friendly Belite-Calcium Sulfoaluminate Cements Obtained from Special Wastes. Applied Sciences-Basel, 10(23).
Tole, I., Habermehl-Cwirzen, K. and Cwirzen, A., 2019. Mechanochemical activation of natural clay minerals: an alternative to produce sustainable cementitious binders—review. Mineralogy and Petrology, 113(4): 449–462.
Statistics Estonia, 2009, 2019, 2020. https://www.stat.ee/
Statistical Yearbook of Estonia 2010. https://www.stat.ee/sites/default/files/2020-08/Aastaraamat_2010_2.pdf
Uibu, M., Kuusik, R., Andreas, L. and Kirsimäe, K., 2011. The CO2-binding by Ca-Mg-silicates in direct aqueous carbonation of oil shale ash and steel slag. 10th International Conference on Greenhouse Gas Control Technologies, 4: 925–932.

Uibu, M., Kuusik, R. and Veskimae, H., 2008a. Seasonal binding of atmospheric CO(2) by oil shale ash. Oil Shale, 25(2): 254–266.
Uibu, M., Somelar, P., Raado, L.M., Irha, N., Hain, T., Koroljova, A. and Kuusik, R., 2016. Oil shale ash based backfilling concrete—Strength development, mineral transformations and leachability. Construction and Building Materials, 102: 620–630.
Uibu, M., Tamm, K., Velts-Janes, O., Kallaste, P., Kuusik, R. and Kallas, J., 2015. Utilization of oil shale combustion wastes for PCC production: Quantifying the kinetics of Ca(OH)(2) and CaSO4 center dot 2H(2)O dissolution in aqueous systems. Fuel Processing Technology, 140: 156–164.
Uibu, M., Tamm, K., Viires, R., Reinik, J., Somelar, P., Raado, L., Hain, T., Kuusik, R. and Trikkel, A., 2021. The composition and properties of ash in the context of the modernisation of oil shale industry. Oil Shale, 38(2): 155–176.
Uibu, M., Trikkel, A. and Kuusik, R., 2007. Transformations in the solid and liquid phase at aqueous carbonization of oil shale ash. Ecosystems and Sustainable Development Vi, 106: 473–482.
Uibu, M., Uus, M. and Kuusik, R., 2009. CO2 mineral sequestration in oil-shale wastes from Estonian power production. Journal of Environmental Management, 90(2): 1253–1260.
Uibu, M., Velts, O., Trikkel, A. and Kuusik, R., 2008b. Reduction of CO(2) emissions by carbonation of alkaline wastewater. Air Pollution Xvi, 116: 311–320.
Usta, M.C., Yoruk, C.R., Hain, T., Paaver, P., Snellings, R., Rozov, E., Gregor, A., Kuusik, R., Trikkel, A. and Uibu, M., 2020. Evaluation of New Applications of Oil Shale Ashes in Building Materials. Minerals, 10(9).
Velts, O., Kindsigo, M., Uibu, M., Kallas, J. and Kuusik, R., 2014. CO2 mineralisation: Production of CaCO3-type material in a continuous flow disintegrator-reactor. 12th International Conference on Greenhouse Gas Control Technologies, Ghgt-12, 63: 5904–5911.
Velts, O., Uibu, M., Kallas, J. and Kuusik, R., 2011. Waste oil shale ash as a novel source of calcium for precipitated calcium carbonate: Carbonation mechanism, modeling, and product characterization. Journal of Hazardous Materials, 195: 139–146.
Velts, O., Uibu, M., Rudjak, I., Kallas, J. and Kuusik, R., 2009. Utilization of oil shale ash to prepare PCC: leachibility dynamics and equilibrium in the ash-water system. Greenhouse Gas Control Technologies 9, 1(1): 4843–4850.
Winnefeld, F. and Lothenbach, B., 2010. Hydration of calcium sulfoaluminate cements—Experimental findings and thermodynamic modelling. Cement and Concrete Research, 40(8): 1239–1247.
Wu, Y.H. and Anthony, E.J., 2011. Investigation of sulphation behavior of two fly ash samples produced from combustion of different fuels in a 165 MWe CFB boiler. Powder Technology, 208(1): 237–241.
Yue, G.X., Cai, R.X., Lu, J.F. and Zhang, H., 2017. From a CFB reactor to a CFB boiler—The review of R&D progress of CFB coal combustion technology in China. Powder Technology, 316: 18–28.

SUMMARY IN ESTONIAN

Põlevkivi keevkihtpõletuse lendtuhk alternatiivsete sideainete toormena

Eesti energeetika tugisambaks on viimased 70 aastat olnud põlevkivi, mis on Ordoviitsiumi-vanuseline mereline orgaanilise aine rikas mudakivim – kukersiit. Selle ulatuslikuimad varud levivad Kirde-Eestis ja Loode-Venemaal Balti Paleobasseini põhjanõlval (Bauert ja Kattai, 1997). Kukersiit on võrreldes teiste maailmas leiduvate põlevkividega suhtelist kõrge energeetilise väärtusega (8–9 MJ/kg) ja Eesti põlevkivi on olnud siiani suurim tööstuslikult kasutatav põlevkiviressurss maailmas (Ots, 2006).

Kuni viimaste aastateni moodustas 70–80% kogu Eesti energiasektorist põlevkivienergeetika ning veel 2007. aastal toodeti üle 90% elektrist põlevkivielektrijaamades (Eesti statistika aastaraamat, 2009). Kui 1980. aastate esimeses pooles kaevandati aastas umbes 20–30 Mt põlevkivi, siis põlevkivi kaevandamine ja selle kasutamine otsepõletuseks elektrijaamades on viimastel aastakümnetel märkimisväärselt vähenenud ning 2019. aastal kaevandati ca. 12 Mt põlevkivi (Eesti Statistika, 2019). Kuigi õlitööstuse osakaal põlevkivikasutuses üha suureneb, siis ka täna läheb sellest suurem osa otsepõletamisele (ligikaudu 70–80% põlevkivist). Ülejäänud kaevandatud põlevkivi leiab kasutust põlevkiviõli tootmises ning kuni 2020. aastani kasutati põlevkivi kütusena ka tsemendi tootmisel.

Põlevkivi põletamisel ning põlevkiviõli tootmisel tekib suurel hulgal tahkeid tuhajäätmeid (ca. 45–53% põlevkivi kuivmassist) (Bauert ja Kattai, 1997). See tähendab, et ka langenud kaevandamise ja elektritootmise mahtude juures tekib igal aastal 6–8 Mt tahkeid jäätmeid, mis teeb Eestist vaieldamatult ühe maailma suurima jäätmetekitaja ühe elaniku kohta (ca. 4–5 t/aastas per capita).

Põlevkivitööstuse tahkete jäätmete võimalikku taaskasutamist on põhjalikult uuritud enam kui 70 aasta jooksul, alates põlevkivi laiema kasutuse algusest (Kattai et al., 2000; Ots, 2006). Varasema tolmpõletus tehnoloogia katelde tuha peenfraktsioone kasutati edukalt põlevkivituhk-tsemendi tootmiseks ja tuha jämedaid fraktsioone (nn tsüklontuhka) tuhaplokkide valmistamisel, aga ka teede aluspinnaste stabiliseerimiseks ning happeliste muldade lupjamiseks. Isegi siis ei ületanud tuha taaskasutus 10% osakaalu (Kuusik et al., 2006).

Ringmajanduse põhimõtete juurdumise taustal on viimase 20 aasta jooksul tehtud põhjalikke uuringuid tuha võimalikuks taaskasutuseks erinevates alternatiivsetes valdkondades, sh nii ehitusmaterjalide tootmisel, plasti täiteainena, sadestatud karbonaadi valmistamiseks ja fosforiärastuse filtermaterjalidena märgalapuhastites (nt. Kõiv et al., 2010; Uibu et al., 2021 jpt.). Vaatamata nendes uuringutes tehtud tohututele jõupingutustele on põlevkivituha taaskasutamine jäänud piiratuks, moodustades vähem kui 2% tekkivast tuha kogusest ja seda isegi praeguste madalate tootmismahtude juures (Paaver et al., 2021—PAPER III). Selle tulemusena ladestatakse igal aastal miljoneid tonne tuhka suurtesse, kuni

45 m kõrgustesse jäätmehoidlatesse, mis hõivavad kahe Eesti suurema elektrijaama kõrval rohkem kui 20 km^2 pindala (Leben et al., 2019).

Tuha võimalikku taaskasutust on olulisel määral piiranud alates 2004. aastast toimunud järk-järguline üleminek vana tüüpi tolmpõletuskateldelt, kus põlemine toimus kõrgetel temperatuuridel (>1200–1400°C), tõhusamatele ja madalama CO_2 heitmega keevkihtkateldele, kus põletamine toimub madalamatel temperatuuridel (800–850°C) (Ots, 2006). Madalam põletamistemperatuur võimaldab drastiliselt vähendada SO_2 emissioone tänu reaktsioonidele vaba lubjaga (CaO), milles tekib tahke Ca-sulfaadi faas anhüdriit ($CaSO_4$) (Anthony, 1995).

Kuigi keevkihis põletamise madalamad temperatuurid tõstavad katelde energiatõhusust ja on madalamate emissioonidega, siis mõjutab sellest tulenev väiksem karbonaatide lagunemisaste ja kõrgem Ca-sulfaadi sisaldus negatiivselt põlevkivituha füüsikalisi kui keemilisi omadusi (Pihu et al., 2012; Raado et al., 2014b; Usta et al., 2020—PAPER I). Võrreldes vanade tolmpõletustuhkadega moodustub selles tuhas oluliselt vähem sekundaarseid kõrgetemperatuurilisi tsementeeruvate omadustega kaltsiumsilikaatseid mineraale. See tähendab, et uued tuhad on oluliselt madalamate ise-tsementeeruvate ja putsolaansete omadustega. Sellised muutused tuha omadustes tekitavad juba täna probleeme tuhajäätmete platoodele ladustamisega (Pihu et al., 2012) ja vähendavad tuha potentsiaalseid taaskasutusviise (Usta et al., 2020—PAPER I).

Eesti põlevkivitööstus on jõudnud oma lõppvaatusesse. Põlevkivielektri osakaal on 2000. aastate esimesest kümnendist järk-järgult vähenenud, kuid alates 2018. aastast on toimunud järsk langus, mille käigus põlevkivielektri osakaal kukkus kahe aastaga 76%-lt vaid 40%-le 2020. aastal (Eesti Statistika, 2020). Põlevkivielektri osakaalu vähenemine energeetikasektoris on otseselt tingitud Euroopa Liidu CO_2 saastekvootide maksustamise poliitikast, mis muudab fossiilkütused energiaturul konkurentsivõimetuks. Samas on sellel protsessil tuntav positiivne tulem Eesti CO_2 heitmete vähenemisele, mille peamine allikas (kuni viimase ajani üle 70%) on põlevkivienergeetika (Eesti Statistika, 2020).

Pidades silmas Euroopa Liidu kliimamuutustega seotud eesmärke ja poliitikat, on tänase Eesti valitsuse koalisatsioonilepingus välja kuulutatud, et põlevkivi kasutamine elektrijaamades peaks lõppema hiljemalt 2035. aastaks ja põlevkiviõli tootmine hiljemalt 2045. aastaks. Veelgi enam, Eesti suurim energiaettevõte Eesti Energia AS teatas, et põlevkivi kasutamine elektrijaamades lõpetatakse juba 2030. aastaks (Eesti Energia, 2021).

Sellegipoolest püsivad põlevkivitööstusega seotud jäätmeprobleemid Eestis ja ka teistes sarnaseid tahkeid kütuseid kasutatavates riikides veel aastakümneid. Samuti jääb jätkuvalt püsima vajadus ladestada või eelistatult taaskasutada teisi leeliselisi tahked jäätmed teistest tööstusharudest, nagu biomassi ja olmejäätmete tuhkasid, terasetööstuse räbu ja tsementitööstuse jäätmeid—mida kõike võiks tulevikus kasutada ringmajanduses alternatiivsete sideainete ja ehitusmaterjalide tootmiseks (Gosh ja Kumar, 2020).

Eriti terav on surve tsementitööstusele, mis toodab umbes 8% maailmas tekkivatest CO_2 heitmetest. Seepärast püütakse leida alternatiive harilikule portlandtsemendile. Sellisteks potentsiaalseteks alternatiivideks peetakse osalise või

täieliku tsemendi aseainena mitmeid erinevaid lendtuhkasid. Kuigi vähese kaltsiumisisaldusega ränirikkaid tuhkasid on juba pikalt uuritud ja need leiavad kasutust segudes koos tavalise tsemendiga või leelisaktiveeritud sideainetes, siis kaltsiumirikkad keevkihtkatelde tuhad, nagu näiteks Eesti põlevkivituhk, ei ole siiamaani leidnud laiemat kasutust oma nõrkade tsementeerumisomaduste ja varieeruva koostise tõttu. Üksvõimalus tõsta selliste tuhkade taaskasutuspotensiaali on nende omaduste muutmine mehaanilise- ja/või leelisaktivatsiooni teel.

Käesolevas doktoritöös uuriti põlevkivi elektrijaamade keevkihtkatelde ning õlitööstuse tahkesoojuskandja lendtuhkade tsementeeruvaid omadusi ning mehaanilise ja leelisaktivatsiooniga modifitseeritud lendtuha uusi kasutusvõimalusi alternatiivse sideainena portlandtsemendile.

Uuringu peamisteks eesmärkideks oli:

- iseloomustada Eesti põlevkivi keevkihttuhkade koostist ja hüdratiseeritud segude mehaanilisi omadusi;
- analüüsida keevkihtkatelde lendtuhkade kasutatavust leelisaktiveeritud ehitusmaterjalidena;
- selgitada mehhaanilise aktivatsiooni mõju keevkihttuhkade hüdratiseerumisele ja sellest valmistatud segude survetugevuse kujunemisele;
- välja töötada mehaaniliselt aktiveeritud põlevkivituha, tsemendi ja liiva baasil tsementeeruvad segud.

Töö tulemused näitavad, et keevkihtkatelde ja Enefit280 õlitehase tuhad on ainult osaliselt dekarboneeritud ning sisaldavad võrreldes varasemate kõrgetemperatuuriliste tolmpõletuskatelde tuhaga oluliselt vähem vaba lupja, sekundaarseid Ca-Mg silikaate ja klaasifaasi, mistõttu on tuhad madalamate putsolaansete omadustega. Võrreldes tolmpõletustuhkadega on potentsiaalsete tsementeeruvate faaside sisaldus keevkihtkatelde tuhkades olenevalt tuha tüübist kaks kuni kolm korda madalam. Kui välja arvata Auvere elektrijaama elektrostaatilistest filtritest kogutud lendtuhk, siis on kõigil teistel tuhatüüpidel madalad ise-tsementeerumisomadused ja nende survetugevused jäävad reeglina alla 10 Mpa. See tähendab, et need tuhad vajavad ehitussektoris kasutamiseks füüsikalis-keemilist või termilist eeltöötlust ja/või segamist teiste tsementeeruvate materjalidega.

Üheks Eesti põlevkivituhkade aktiviseerimise võimalikuks viisiks on leelisaktivatsioon, milles Si ja Al-rikaste faaside polümeriseerumisel aluselises keskkonnas moodustuvad kolmedimensionaalsed võrgustikud ning tekivad kõrge survetugevusega ning keemilisest vastupidavad sideained/materjalid, mis sobivad kasutamiseks erinevates ehitusvaldkondades. Kuigi Eesti kaltsiumirikaste põlevkivituhkade leelisaktiveerimisel käivituvad polümerisatsioonireaktsioonid ning moodustuvad C-(A)-S-H tüüpi struktuurid, siis nende tuhkade potentsiaal geopolümeeride valmistamiseks on madal või puudub täielikult. Võrreldes teiste tööstuslike jäätmematerjalidega, mida kasutatakse leelisaktiveeritud sideainete, täpsemalt geopolümeeride tootmiseks, on Ca-rikas põlevkivituhas oluliselt vähem reaktiivset räni ja alumiiniumit, mis on vajalik Si-Al polümeersete võrkude

moodustamiseks. Polümeerseid võrgustikke koordineerivate leeliselementide sisaldus põlevkivituhas on küll kõrge, aga polümeriseerimisreaktsioonid on piiratud. Erinevate tuhkade leelisaktivatsioonil küündivad kõrgeimad survetugevused ca. 12 MPa tasemele. Lisaks iseloomustab Eesti põlevkivituha leelisaktiveeritud materjale tugev mahukahanemine, mis põhjustab ulatuslike mikropragude tekkimise ning materjali nõrgenemise pikaajalisel seismisel.

Samas parandas Ca-rikka põlevkivi keevkiht lendtuha mehaaniline aktiviseerimine olulisel määral tuhasegude tsementeerumist. Juba lühiajaline jahvatamine (2–4 min) parandas katsekehade survetugevusi mitmekordselt, saavutades 90 päeva kuivamise jooksul tugevuse 60 MPa ilma igasuguse keemilise aktiveerimise või muude lisanditeta. Sama tuha puhul saavutati ilma aktiviseerimiseta 90 päevaga maksimaalseks survetugevuseks vaid 9 MPa. Mehaaniline aktiveerimine jahvatamise teel suurendab oluliselt tuha eripinda ja vähendab keskmist terasuurust, lõhkudes keevkihttuhkadele iseloomulikke suuri ebakorrapärased tuhaosakeste känkraid, sh komplekssseid reageerimata vaba CaO südamikega $CaSO_4$ sfääruleid. Selle protsessi tulemusena kasvab tuhkade reaktiivsus ja võime moodustada tugevaid tsementeeruvaid sidemeid.

Mehaaniliselt aktiveeritud keevkihituhaga valmistatud hüdratiseeritud materjali tsementeerumisomadusi kontrollib peamiselt Ca-sulfoaluminaat faasi—etringiidi ($Ca_6Al_2(OH)_{12}(SO_4)_3 \cdot 26H_2O$)—moodustumine. Ettringiit tekitab tiheda läbi põimunud nõeljate kristallide võrgustiku, mis annab esmase tsementeeruvuse ja juba 7 päeva möödumisel on materjali survetugevused >30 MPa. Tsementeerumise hilisematel etappidel hakkab Ca-hüdroksiidi karboniseerumisel pooriruumis moodustumakaltsiit ning leeliselises poorikeskkonnas ka täiendav amorfsest heterogeenne Ca-Al-Si C-(A)-S-H geel, mis annavad materjalile täiendava mehhaanilise tugevuse. Ettringiidi moodustumist põlevkivituhas mõjutab lahustunud kaltsiumi, sulfaadi ja ennekõike alumiiniumi kättesaadavus, mille peamisteks allikateks on Al sisaldavate faaside (klaas, savimineraalid, päevakivid) lahustumine aluselises keskkonnas. Ettringiit moodustub ka aktiveerimata tuhas, kuid erinevalt jahvatatud tuhast, kus peenendatud tuhast tekib tihe kompaktne struktuur, kasvavad aktiveerimata tuhas ettringiidi kristalliidid pooriruumi ning osakeste sidustumine jääb nõrgemaks.

Aktiveeritud kaltsiumirikastest lendtuhkadest valmistatud materjalide keemiline ja mineraalne koostis ning tsementeerumisprotsess on sarnased kaltsiumsulfoaluminaat-tsementidega (CSA), kus hüdratiseerunud segude tsementeerumine sõltub peamiselt ye'elimiidi ja kipsi hüdratatsioonist, mille tulemusel tekivad ettringiit ja nanokristalne Al-hüdroksiid. CSA tsemente peetakse üheks võimalikuks tavalise portlandtsemendi alternatiiviks ning nendeks on kasutatavad ka Ca- ja väävlirikkad keevkiht katelde tuhad. Sellele viitab ka aktiveeritud keevkihttuha käitumine segudes koos hariliku portlantsemendiga. Kui aktiveerimata keevkiht lendtuhk käitub segudes tsemendiga pigem inertse täiteainena ning segude survetugevused langevad proportsionaalselt koos tuha osakaalu suurenemisega, siis mehaaniliselt aktiveeritult lendtuhk toimib hoopis aktiivse sideainena ja võimaldab suurtes mahtudes portlandtsemendi asendamist. Katsekehad, milles tsement oli kuni 50% ulatuses mehaaniliselt aktiveeritud lendtuhaga asendatud,

saavutasid 7 ja 28 päeva jooksul peaaegu sama kõrge survetugevuse kui puhtast portlandtsemendist valmistatud katsekehad. Survetugevuste erinevused olid reeglina väiksemad kui 10%, mis viitab võimalusele, et tulevikus võiks mehaaniliselt aktiveeritud lendtuhka edukalt kasutada Ca-sulfoaluminaat tsemendi tüüpi sideainena. Samuti kiirendab aktiveeritud keevikihikatelde lendtuha tsemendisegusse lisamine esmase survetugevuse saavutamist, mis võimaldaks nende segude kasutamist erinevates parandustöödes või rakendustes, kus vajatakse kiiret kivinemist.

ACKNOWLEDGEMENTS

I would especially like to thank my supervisors for all their help and support with the thesis. I would also like to thank my co-authors, all the PhD students and staff in the department of geology for all the help, hard work and contributions, Gunnar Nurk for TGA analysis, Estonian Energy for the provided raw materials and Choosday-design for producing essential custom-made laboratory equipment.

PUBLICATIONS

CURRICULUM VITAE

Name: Peeter Paaver
Date of birth: 20.09.1992
Address: Department of Geology, Institute of Ecology and Earth Sciences, University of Tartu,
Ravila 14A, 50411 Tartu, Estonia
Contact: +372 5693 6545
E-mail: peeter.paaver@ut.ee

Education:

2017–…	University of Tartu, Department of Geology, PhD student in environmental technology
2014–2016	University of Tartu, MSc in geology
2011–2014	University of Tartu, BSc in geology

Professional employment:

2017–…	Junior Research Fellow of Geology, University of Tartu, Department of Geology
2014–2017	Analyst, University of Tartu, Department of Geology
2014	Specialist in Geology, University of Tartu, Department of Geology
2012–2014	Laboratory Assistant in Geology, University of Tartu, Department of Geology

Field of research: Natural Sciences and Engineering; Process Technology and Materials Science; Material technology.

Publications:

I **Paaver, P**; Paiste, P; Kirsimäe, K (2016). Geopolymeric potential of Estonian oil shale solid residues: Petroter solid heat carrier retorting ash. Oil Shale, 33 (4), 373−392. DOI: 10.3176/oil.2016.4.05.

II **Paaver, P;** Paiste, P; Mõtlep, R; Kirsimäe, K (2017). Self-cementation and alkali activation of Enefit280 solid heat carrier retorting ash. Oil Shale, 37 (3), 263−278. DOI: 10.3176/oil.2017.3.05.

III **Paaver, P**.; Paiste, P.; Liira, M.; Kirsimäe, K. (2019). Alkali activation of Estonian Ca-rich oil shale ashes: a synthesis. *Oil Shale*, 36, 214−225. DOI: 10.3176/oil.2019.2S.11..

IV Leben, Kristjan; Mõtlep, R; **Paaver, P**; Alar K; Pihu, T; Paiste, P; Heinmaa, I; Nurk, G; Anthony, E; Kirsimäe, K (2019). Long-term mineral transformation of Ca-rich oil shale ash waste. The Science of The Total Environment, 658, 1404−1415. DOI: 10.1016/j.scitotenv.2018.12.326.

V Paiste, P.; Külaviir, M.; **Paaver, P**.; Heinmaa, I.; Vahur, S.; Kirsimäe, K. (2019). Beneficiation of oil shale processing waste: secondary binder phases in alkali activated composites. Waste and Biomass Valorization, 1−11. DOI: 10.1007/s12649-017-0140-6.

VI Leben, K; Mõtlep, R; **Paaver, P**; Konist, A; Pihu, T; Kirsimäe, K (2020). Geochemical study of stable carbon and oxygen isotopes in landfilled Ca-rich oil shale ash. Estonian Journal of Earth Sciences, 69 (3), 134−142. DOI: 10.3176/earth.2020.09.

VII Berber, H.; Tamm, K.; Leinus, M-L.; Kuusik, R.; Tõnsuaadu, K.; **Paaver, P.;** Uibu, M. (2020). Accelerated carbonation technology granulation of industrial waste: Effects of mixture composition on product properties. Waste, Management & Research: The Journal for a Sustainable Circular Economy, 38 (2), 142−155. DOI: 10.1177/0734242X19886646.

VIII Usta, M.C.; Yoruk, C.R.; Hain, T.; **Paaver, P**.; Snellings, R.; Rozov, E.; Gregor, A.; Kuusik, R.; Trikkel, A.; Uibu, M. (2020). Evaluation of new applications of oil shale ashes in building materials. *Minerals*, 10, 765. DOI: 10.3390/min10090765.

IX **Paaver, P**.; Paiste, P.; Liira, M.; Kirsimäe, K. (2021). Mechanical activation of the Ca-rich circulating fluidized bed combustion fly ash: development of an alternative binder system. *Minerals* 11, 3. DOI: 10.3390/min11010003.

X **Paaver, P**.; Järvik, O.; Kirsimäe, K. (2021). Design of high volume CFBC fly ash based calcium sulfoaluminate type binder in mixtures with ordinary Portland cement. Manuscript submitted to *Materials*.

ELULOOKIRJELDUS

Nimi: Peeter Paaver
Sünniaeg: 20.09.1992
Aadress: geoloogia osakond, ökoloogia ja maateaduste instituut, Tartu Ülikool,
Ravila 14A, 50411 Tartu, Eesti
Kontakt: +372 5693 6545
E-post: peeter.paaver@ut.ee

Haridus:

2017–…	Tartu Ülikool, Geoloogia osakond, keskkonnatehnoloogia doktorant
2014–2016	Tartu Ülikool, MSc geoloogias
2011–2014	Tartu Ülikool, BSc geoloogias

Teenistuskäik:

2017–…	Tartu Ülikool, Geoloogia osakond, geoloogia nooremteadur
2014–2017	Tartu Ülikool, Geoloogia osakond, analüütik
2014	Tartu Ülikool, Geoloogia osakond, geoloogia spetsialist
2012–2014	Tartu Ülikool, Geoloogia osakond, laborant

Teadustöö põhisuunad: Loodusteadused ja tehnika; Protsessitehnoloogia ja materjaliteadus; Materjalitehnoloogia.

Publikatsioonid:

I **Paaver, P**; Paiste, P; Kirsimäe, K (2016). Geopolymeric potential of Estonian oil shale solid residues: Petroter solid heat carrier retorting ash. Oil Shale, 33 (4), 373−392. DOI: 10.3176/oil.2016.4.05.

II **Paaver, P;** Paiste, P; Mõtlep, R; Kirsimäe, K (2017). Self-cementation and alkali activation of Enefit280 solid heat carrier retorting ash. Oil Shale, 37 (3), 263−278. DOI: 10.3176/oil.2017.3.05.

III **Paaver, P**.; Paiste, P.; Liira, M.; Kirsimäe, K. (2019). Alkali activation of Estonian Ca-rich oil shale ashes: a synthesis. *Oil Shale*, 36, 214−225. DOI: 10.3176/oil.2019.2S.11..

IV Leben, Kristjan; Mõtlep, R; **Paaver, P**; Alar K; Pihu, T; Paiste, P; Heinmaa, I; Nurk, G; Anthony, E; Kirsimäe, K (2019). Long-term mineral transformation of Ca-rich oil shale ash waste. The Science of The Total Environment, 658, 1404−1415. DOI: 10.1016/j.scitotenv.2018.12.326.

V Paiste, P.; Külaviir, M.; **Paaver, P**.; Heinmaa, I.; Vahur, S.; Kirsimäe, K. (2019). Beneficiation of oil shale processing waste: secondary binder phases in alkali activated composites. Waste and Biomass Valorization, 1−11. DOI: 10.1007/s12649-017-0140-6.

VI Leben, K; Mõtlep, R; **Paaver, P**; Konist, A; Pihu, T; Kirsimäe, K (2020). Geochemical study of stable carbon and oxygen isotopes in landfilled Ca-rich oil shale ash. Estonian Journal of Earth Sciences, 69 (3), 134−142. DOI: 10.3176/earth.2020.09.

VII Berber, H.; Tamm, K.; Leinus, M-L.; Kuusik, R.; Tõnsuaadu, K.; **Paaver, P.;** Uibu, M. (2020). Accelerated carbonation technology granulation of industrial waste: Effects of mixture composition on product properties. Waste, Management & Research: The Journal for a Sustainable Circular Economy, 38 (2), 142−155. DOI: 10.1177/0734242X19886646.

VIII Usta, M.C.; Yoruk, C.R.; Hain, T.; **Paaver, P**.; Snellings, R.; Rozov, E.; Gregor, A.; Kuusik, R.; Trikkel, A.; Uibu, M. (2020). Evaluation of new applications of oil shale ashes in building materials. *Minerals*, 10, 765. DOI: 10.3390/min10090765.

IX **Paaver, P**.; Paiste, P.; Liira, M.; Kirsimäe, K. (2021). Mechanical activation of the Ca-rich circulating fluidized bed combustion fly ash: development of an alternative binder system. *Minerals* 11, 3. DOI: 10.3390/min 11010003.

X **Paaver, P**.; Järvik, O.; Kirsimäe, K. (2021). Design of high volume CFBC fly ash based calcium sulfoaluminate type binder in mixtures with ordinary Portland cement. Manuscript submitted to *Materials*.

DISSERTATIONES TECHNOLOGIAE CIRCUMIECTORUM UNIVERSITATIS TARTUENSIS

1. **Sille Teiter.** Emission rates of N_2O, N_2, CH_4 and CO_2 in riparian grey alder forests and subsurface flow constructed wetlands. Tartu, 2005, 134 p.
2. **Kaspar Nurk.** Relationships between microbial characteristics and environmental conditions in a horizontal subsurface flow constructed wetland for wastewater treatment. Tartu, 2005, 123 p.
3. **Märt Öövel.** Performance of wastewater treatment wetlands in Estonia. Tartu, 2006, 148 p.

   Sergei Yurchenko. Determination of some carcinogenic contaminants in food. Tartu, 2006, 143 p. Published in *Dissertation Chimicae Universitatis Tartuensis,* 51.
4. **Alar Noorvee.** The applicability of hybrid subsurface flow constructed wetland systems with re-circulation for wastewater treatment in cold climates. Tartu, 2007, 117 p.

   Ülle Jõgar. Conservation and restoration of semi-natural floodplain meadows and their rare plant species. Tartu, 2008, 99 p. Published in *Dissertation Biologicae Universitatis Tartuensis*, 139.
5. **Christina Vohla.** Phosphorus removal by various filter materials in subsurface flow constructed wetlands. Tartu, 2008, 103 p.
6. **Martin Maddison.** Dynamics of phytomass production and nutrient standing stock of cattail and its use for environment-friendly construction. Tartu, 2008, 87 p.
7. **Marika Truu.** Impact of land use on microbial communities in Estonian soils. Tartu, 2008, 126 p.
8. **Elar Põldvere.** Removal of organic material, nitrogen and phosphorus from wastewater in hybrid subsurface flow constructed wetlands. Tartu, 2009, 107 p.
9. **Margit Kõiv.** Treatment of landfill leachate and municipal wastewater in subsurface flow filters using mineralized peat and hydrated oil shale ash. Tartu, 2010, 147 p.
10. **Jaanis Juhanson.** Impact of phytoremediation and bioaugmentation on the microbial community in oil shale chemical industry solid waste. Tartu, 2010, 95 p.

    Aare Selberg. Evaluation of environmental quality in Northern Estonia by the analysis of leachate. Tartu, 2010, 117 p. Published in *Dissertation Chimicae Universitatis Tartuensis,* 99.
11. **Riho Mõtlep.** Composition and diagenesis of oil shale industrial solid wastes. Tartu, 2010, 127 p.
12. **Igor Zaytsev.** Bioaugmentation in LWA-filled horizontal subsurface flow filters for wastewater treatment: Impact of flow regime, temperature and donor system Tartu, 2010, 97 p.

13. **Siiri Velling.** Microbial BOD biosensor for wastewater analysis. Tartu, 2011, 79 p.
14. **Riina Lepik.** Biodegradability of phenolic compoundsas single and mixed substrates by activated sludge. Tartu, 2011, 153 p.
15. **Liis Marmor.** Ecology and bioindicative value of epiphytic lichens in relation to air pollution and forest continuity. Tartu, 2011, 98 p.
16. **Martin Liira.** Active filtration of phosphorus in Ca-rich hydrated oil shale ash: precipitation mechanisms and recovery. Tartu, 2012, 84 p.
17. **Kristjan Karabelnik.** Advanced design and management of hybrid constructed wetlands: environmental and water purification effects. Tartu, 2012, 128 p.
18. **Hiie Nõlvak.** Influence of qPCR workflow on target gene enumeration from environmental samples in the case of bioremediation potential estimation. Tartu, 2012, 136 p.
19. **Merlin Raud.** Study of semi-specific BOD biosensors for biosensor-array. Tartu, 2013, 103 p.
20. **Ivar Zekker.** Enrichment of anaerobic ammonium oxidizing bacteria for nitrogen removal from digester effluent and anammox process acceleration by intermediate compounds. Tartu, 2013, 142 p.
21. **Annika Uibopuu**. Communities of arbuscular mycorrhizal fungi in spruce forest ecosystem and their effect on performance of forest understorey plant species. Tartu, 2013, 104 p.
22. **Jekaterina Jefimova.** Leaching of polycyclic aromatic hydrocarbons (PAHs) and heavy metals from the oil shale processing wastes and from waste-based products. Tartu, 2015, 184 p.
23. **Teele Ligi**. Bacterial community structure and its genetic potential for nitrogen removal in the soils and sediments of a created riverine wetland complex. Tartu, 2015, 127 p.
24. **Kuno Kasak**. Greenhouse gas emissions and water treatment efficiency in subsurface flow filters using various substrates. Tartu, 2016, 128 p.
25. **Martin Ligi**. Application of close range remote sensing for monitoring aquatic environment. Tartu, 2017, 146 p.
26. **Mikk Espenberg.** Impact of management on peatland microbiome and greenhouse gas emissions. Tartu, 2017, 152 p.
27. **Jens-Konrad Preem.** Forest soil bacterial community analysis using high-throughput amplicon sequencing. Tartu, 2017, 108 p.
28. **Taavi Vaasma.** Enrichment, atmospheric dispersion and deposition of naturally occurring radionuclides from oil shale-fired power plants. Tartu, 2017, 175 p.
29. **Kristjan Oopkaup.** Microbial community and its relationship with pollutant removal in treatment wetlands. Tartu, 2018, 154 p.
30. **Ergo Rikmann.** Autotrophic nitrogen removal and relevant equilibrial processes. Tartu, 2019, 179 p.

31. **Kati Klein.** Studies and treatment of inhibitory and recalcitrant wastewater. Tartu, 2021, 168 p.
32. **Thomas Schindler.** Tree stem CH_4 and N_2O fluxes in various forest ecosystems. Tartu, 2021, 182 p.